

CIRRCULUM VITAE
Cooper E. Roache

Email contact: croache129@gmail.com

EDUCATION

University of Maryland, Baltimore – Graduate School

M.S., Cellular and Molecular Biomedical Sciences, December 2021
Baltimore, MD

University of Maryland, College Park

B.A., Philosophy (Supporting Area in Neuropsychology), May 2016
College Park, MD

Howard Community College

A.A., General Studies Science Emphasis, June 2017
Columbia, MD

PROFESSIONAL EXPERIENCE

University of Maryland, Baltimore – Department of Physiology

Laboratory Technician/Master's Student, November 2020 – Present
Baltimore, MD

- Write animal use protocols including purpose/significance of research, statistical power calculations and experimental design flow in compliance with university IACUC standards and regulation
- Design and conduct experimental behavioral assays in mouse models of KCNMA1-linked Channelopathy for evaluation of motor function
- Perform statistical analysis and graph development of all behavioral assay data using Prism GraphPad
- Program original Python 3 scripts to perform multi-parameter analysis of mouse wheel activity
- Maintain experimental rodent colony, laboratory functions and budgetary reallocations

University of Maryland, Baltimore – School of Medicine

Comparative Medical Research Assistant, July 2018 – November 2020
Baltimore, MD

- Wrote and reviewed standard operating procedures outlining the Comparative Medicine Sentinel Program in compliance with the university quality assurance
- Reviewed and amended budgetary estimates for research protocols according to proper service and medical/material resource requirements

- Assisted in study conduct with non-sedate NHP's for cobalt-60 γ -radiation LD-50 mortality study
- Served as surgical technician for swine hindlimb ischemia and reperfusion study
- Collected tissue and blood samples from RAP/MAP, quarantine and sentinel rodents for purposes of facility pathology diagnostics
- Served as clinical technician for on-call medical treatment and assistance

Freetown Animal Hospital

Primary Surgical Assistant, August 2017 – August 2019

Columbia, MD

- Served as surgical assistant in all anesthetic procedures – conducted CBC/chemistry in-house, administered pre-medication, placed peripheral IV catheter, performed anesthetic induction, placed endotracheal tube and monitored vitals for all procedures
- Trained multiple assistants in effective and medically appropriate anesthetic monitoring and surgical assistance
- Collected, prepared and examined all in-house cytology and diagnostic samples including blood, urine via cystocentesis/urethral catheterization and skin/tumor cytology via fine needle aspirate
- Maintained hospital inventory, all in-hospital diagnostic machinery and client communications/follow-ups

Banfield Pet Hospital

Veterinary Assistant, June 2015 – July 2017

Columbia, MD

- Assisted veterinarians in physical examinations, medical notes, medication preparation and conveyed veterinary medical knowledge and practices to clients in a concise and effective manner
- Published articles educating the public in preventive care practices on behalf of Banfield for local magazines
- Monitored all hospital anesthetic procedures and independently performed dental prophylaxis procedures
- Administered vaccines, collected blood samples, placed IV catheters and assisted in operating radiology/ultrasound equipment

TEACHING EXPERIENCE

University of Maryland, Baltimore County

Lecturer for CMSC 304

Social and Ethical Issues in Information Technology, February 2019

Baltimore, MD

- Wrote/distributed sample essay in classic ethical/persuasive writing for student use and use in future semesters
- Provided general overview of ethical theory and applied ethics as it pertained to information technology
- Conducted both student group discussions on ethical issues and mock debates to model both proper argument structure and common logical fallacies

AWARDS

Annual Graduate Research Conference

University of Maryland, Baltimore, March 2021

Award for Best Oral Presentation, "Assessment of Behavioral Phenotypes in D434G and N999S Mouse Models of *KCNMA1*-linked Channelopathy"

ABSTRACT

Title of Thesis: Evaluation of Motor Function in Mouse Models of *KCNMA1*-linked Channelopathy

Cooper Roache, Master of Science, 2021

Thesis Directed by: Andrea Meredith, Ph.D., Professor, Department of Physiology

KCNMA1-linked channelopathy is a rare neuromuscular disease associated with patient phenotypes of paroxysmal non-kinesigenic dyskinesia (PNKD). The N999S and D434G variants of the BK channel-encoding *KCNMA1* gene currently comprise the largest patient cohorts. Heterologous cellular systems expressing N999S and D434G mutations show gain-of-function property changes, while KO mouse models (*Kcnma1*^{-/-}) show tremors and ataxia associated with increased neuronal excitability of cerebellar Purkinje neurons. Thus, it can be hypothesized that *KCNMA1* variants would cause dyskinesia phenotypes in mice. However, there is a lack of evidence in literature suggesting that BK channel property changes from *KCNMA1* variants cause PNKD patient phenotypes. In this study, mice harboring N999S (*Kcnma1*^{N999S/WT}) and D434G (*Kcnma1*^{D434G/WT}) mutations are exposed to a series of assays evaluating motor function for dyskinesia characteristics. Validation of dyskinesia phenotypes in these mouse models could shape future investigations in molecular mechanisms of genotype-phenotype relations and pharmacologic treatment options.

Evaluation of Motor Function in Mouse Models of *KCNMA1*-linked Channelopathy

by
Cooper E. Roache

Thesis submitted to the Faculty of the Graduate School of the
University of Maryland, Baltimore in partial fulfillment
of the requirements for the degree of
Master of Science
2021

© Copyright 2021 by Cooper E. Roache
All rights reserved

ACKNOWLEDGEMENTS

Thank you to my parents, Eddie Roache and Susan Mitchell, for their support throughout my entire education. Though it may have taken me some time to understand, you inevitably taught me a love for learning and a commitment to thoughtful analysis. Your enthusiasm towards my career path as a veterinary technician and now a researcher has provided great love and motivation.

Thank you to my lab partners, Su Mi Park, Katia Matychak and Ria Dinsdale for all of the encouragement and empathy given to me throughout my thesis work. I have thoroughly enjoyed learning from all of you.

Thank you to my committee members, Dr. Todd Gould and Dr. Junfang Wu, for the use of your behavioral testing equipment and commitment to improving my research process.

Thank you to my program director, Dr. Ivy Dick, former program director, Dr. Selen Catania, and program administrator, Elice Garcia-Baca. All of you have always provided thoughtful accommodations to me throughout my graduate school education.

And finally, thank you to my PI and mentor, Dr. Andrea Meredith. I am so grateful for the opportunity you have given me to be a part of such a wonderful lab and field of research. The trust that you have put in me and my abilities as both your lab technician and a graduate student has given me encouragement throughout my research and for my future endeavors. I have gained an immense understanding of what it takes to conduct thorough and rigorous scientific research. Thank you for all you have done for me.

TABLE OF CONTENTS

ACKNOWLEDGEMENTS	iii
LIST OF TABLES	vi
LIST OF FIGURES	vii
LIST OF ABBREVIATIONS.....	viii
CHAPTER 1: INTRODUCTION.....	1
1.1. Patient PNKD Phenotypes of the Largest Cohorts of KCNMA1-linked channelopathy.....	1
1.2. BK Channel Background and Expression.....	3
1.3. Rodent Models of Dyskinesia	9
1.4. Phenotypes of KCNMA1 Patient Variants in Cellular Expression Systems and Rodent Models	12
CHAPTER 2: SPECIFIC AIMS AND RATIONALE.....	16
2.1. Elicited Motor Function	17
2.2. Spontaneous Motor Function	18
CHAPTER 3: METHODOLOGY	22
3.1. Mice.....	22
3.2. Hanging Wire	22
3.3. Rotarod.....	23
3.4. Gait Analysis (CatWalk XT).....	24
3.5. Free-running Wheel Activity	25
3.6. Restraint-induced Dyskinesia Analysis.....	26
CHAPTER 4: RESULTS.....	28

4.1. Kcnma1 ^{N999S/WT} and Kcnma1 ^{-/-} Show Elicited Motor Impairment.....	28
4.2. Kcnma1 ^{N999S/WT} and Kcnma1 ^{-/-} Mice Show Unique Spontaneous Motor Impairment Suggestive of Dyskinesia.....	34
CHAPTER 5: DISCUSSION.....	44
5.1. General Discussion.....	44
5.2. Future Direction	47
APPENDIX 1: BK CHANNELS EXPRESSION.....	51
APPENDIX 2: DESCRIPTIONS OF DYSKINESIA RODENT MODELS.....	53
APPENDIX 3: ALL CATWALK PARAMETERS AND WEIGHT COMPARISON....	55
APPENDIX 4: REPRESENTATIVE IMAGES AND VIDEO OF RESTRAINT- INDUCED DYSKINESIA BEHAVIOR.....	61
REFERENCES	63

LIST OF TABLES

Table 1.1. Expression of BK channels across movement- and motor-related areas of the central and peripheral nervous system.....	8
Table 1.2. Comparative rodent models of dyskinesia.....	12
Table 1.3. Flow-chart of rotarod assay procedural timeline.	24
Appendix Table 1. BK channel motor phenotype associations in cellular and animal models across the central and peripheral nervous system.	51
Appendix Table 2. Phenotype descriptions in rodent models of baseline and paroxysmal dyskinesias.....	53
Appendix Table 3. Comparison of all significant CatWalk parameters p-values across <i>Kcnma1</i> ^{N999S/WT} , <i>Kcnma1</i> ^{D434G/WT} and <i>Kcnma1</i> ^{-/-} cohorts.....	55

LIST OF FIGURES

Figure 1.1. Expression of BK channels in brain regions associated with motor control, coordination and processing.	5
Figure 4.1. <i>Kcnmal</i> ^{N999S/WT} and <i>Kcnmal</i> ^{-/-} mice show lower fall latency times during elicited motor assays.	29
Figure 4.2. <i>Kcnmal</i> ^{-/-} mice show motor learning deficits.	33
Figure 4.3. <i>Kcnmal</i> ^{N999S/WT} and <i>Kcnmal</i> ^{-/-} mice show gait disturbances in forelimb and hindlimb parameters respectively.	36
Figure 4.4. <i>Kcnmal</i> ^{N999S/WT} and <i>Kcnmal</i> ^{-/-} mice show wheel activity deficits.	39
Figure 4.5. <i>Kcnmal</i> ^{N999S/WT} mice longer immobility time.	43
Appendix Figure 1. <i>Kcnmal</i> ^{-/-} mice show lower weight prior to CatWalk gait capture. .	60
Appendix Figure 2. Representative images of <i>Kcnmal</i> ^{WT/WT} and <i>Kcnmal</i> ^{N999S/WT} mice. .	61
Appendix Video 1. Representative video of <i>Kcnmal</i> ^{N999S/WT} , <i>Kcnmal</i> ^{WT/WT} and <i>Kcnmal</i> ^{-/-} mice.	62

LIST OF ABBREVIATIONS

ACh	acetylcholine
AP	action potential
AHP	afterhyperpolarization
BK	‘big’ potassium channel
<i>CACNA1A</i>	gene encoding calcium voltage-gated channel alpha 1A subunits
<i>C57BL/6J</i>	inbred wild-type strain from Jackson Laboratory
CRISPR	biotechnology used for gene editing
D434G	aspartic acid to glycine <i>KCNMA1</i> patient variant
GOF	gain of function
H444Q	histidine to glutamine <i>KCNMA1</i> patient variant
HD	Huntington’s disease
<i>HTT</i>	huntingtin gene
<i>KCNMA1</i>	gene encoding ‘big’ potassium channel alpha 1 subunits
<i>Kcnma1</i> ^{-/-}	mice lacking BK channels
<i>Kcnma1</i> ^{D434G/WT}	mice harboring a <i>KCNMA1</i> D434G mutation
<i>Kcnma1</i> ^{N999S/WT}	mice harboring a <i>KCNMA1</i> N999S mutation
KO	knockout
LOF	loss of function
N999S	asparagine to serine <i>KCNMA1</i> patient variant
<i>NIPA2</i>	magnesium transporter gene
NMDA	N-methyl-D-aspartate
NMJ	neuromuscular junction

PKD	paroxysmal kinesigenic dyskinesia
PNKD	paroxysmal non-kinesigenic dyskinesia
PNKD3	paroxysmal non-kinesigenic dyskinesia type 3
<i>PNKD</i> mut-Tg	mice harboring a patient <i>PNKD</i> gene mutation
<i>PRRT2</i>	proline-rich transmembrane protein 2 gene
PTZ	pentylenetetrazol
PxD	general (x) paroxysmal dyskinesia
R6	mice harboring a CAG repeat (x6) in the huntingtin gene
R1097H	arginine to histidine <i>KCNMA1</i> patient variant
RIM	Rab3-interacting module
RPM	rotations per minute
SK	‘small’ potassium channel
WT	wild-type

CHAPTER 1: INTRODUCTION

1.1. Patient PNKD Phenotypes of the Largest Cohorts of KCNMA1-linked channelopathy

KCNMA1-linked channelopathy is a rare neuromuscular disease that is associated with varying movements disorders, epilepsy, developmental delays and intellectual disabilities (Bailey et al., 2019). There are currently 37 known patient variants of the *KCNMA1* gene that are associated with these symptoms. The N999S and D434G variants currently comprise the largest cohorts of patients and are associated with abnormal involuntary movements without seizure activity called dyskinesia. Dyskinesia can include, but is not limited to, ataxia, tremors, dystonia (abnormal posturing), chorea (twisting/writhing), hyper/hypokinesia (excessive or lack of movement) and myoclonus (jerking movements). *KCNMA1* patients harboring N999S and D434G variants show symptoms of paroxysmal non-kinesigenic dyskinesia (PNKD) (Bailey et al., 2019; Miller et al., 2021). PNKD is defined by the episodic (paroxysmal) onset and termination of dyskinesia, as opposed to baseline dyskinesias that are continually present like ataxia and tremors. PNKD movements are not provoked by sudden movement (non-kinesigenic). Rather, triggers of some PNKD types can include stress, sleep deprivation, alcohol and/or caffeine (Garone et al., 2020; McGuire et al., 2018). The episodic attacks (paroxysms) show no epileptic EEG activity and patients maintain consciousness (Keros et al., 2021; Miller et al., 2021). The N999S and D434G variants are associated specifically with PNKD type 3. Unlike the paroxysms of PNKD that last minutes to hours and occur a few times a day, PNKD3 paroxysms are shorter and more frequent (hundreds of times per day) (McGuire et al., 2018; Miller et al., 2021).

Though both D434G and N999S variants are associated with PNKD3, they are also associated with other varying characteristics. D434G patients have been associated with both generalized tonic-clonic seizures, involving rapid, involuntary jerking movements, and absence seizures, involving seizure activity associated with immobility (Du et al., 2005). The D434G variant was first reported in a family of thirteen affected individuals with either generalized epilepsy, paroxysmal dyskinesias (PxDs) or both. The individuals carried the heterozygous allelic configuration. It is the only variant to be identified clinically from a patient pedigree and shows autosomal dominant inheritance. It was reported that alcohol was a common trigger of patient dyskinesia paroxysms, which is consistent with some forms of PNKD.

The N999S variant has now been identified in twelve unrelated patients. These N999S patients exhibit similar symptoms to D434G patients including epilepsy, PNKD or both (Miller et al., 2021). Patients also carry the heterozygous allelic configuration of the variant. Unlike the D434G variant, the N999S variant thus far arises *de novo* with no generational inheritance. Early-onset and developmental delays have been reported in N999S patients (Heim et al., 2020; J. Heim, 2019; Wang et al., 2017; Zhang et al., 2015). Paroxysms of both D434G and N999S patients have been described in terms of ‘drop attacks’ in which dyskinetic movements resemble cataplexy (immobility with axial hypotonia and dystonic posturing of extremities) (Du et al., 2005; Heim et al., 2020; J. Heim, 2019; Miller et al., 2021). Excitement, fatigue and general strong emotions have been identified as triggers common to multiple N999S patients (Heim et al., 2020; Keros et al., 2021; Wang et al., 2017). Like D434G patients, three N999S patients have also shown absence seizures (Heim et al., 2020; Li et al., 2018). Though anti-seizure

medications are recommended for treatment, they are not effective in resolving dyskinesia. One N999S patient was found to have paroxysms further provoked by the anti-seizure medication oxcarbazepine (Wang et al., 2017). There is a lack of literature on mechanisms of changes in neuronal activity causing ‘drop attacks’ in *KCNMA1* patients. As such, this has made understanding and characterizing the disease difficult, as well as investigating effective treatment.

1.2. BK Channel Background and Expression

The *KCNMA1* gene encodes the alpha subunit of BK channels – large-conductance voltage- and Ca^{2+} -activated K^+ channels that produce a rapidly activating outward current in response to membrane depolarization and increases in Ca^{2+} concentration (Dworetzky et al., 1994; McCobb et al., 1995; Pallanck and Ganetzky, 1994). In neurons, they are associated with regulation of repolarizing and afterhyperpolarizing (AHP) phases in action potentials (APs) (Faber and Sah, 2002; Fagerberg et al., 2014; Gu et al., 2007; Shao et al., 1999). BK channels are also associated with regulation of Ca^{2+} influx that signal pre-synaptic neurotransmitter release and synaptic plasticity of dendrites (Misonou et al., 2006; Raffaelli et al., 2004; Rancz and Hausser, 2006).

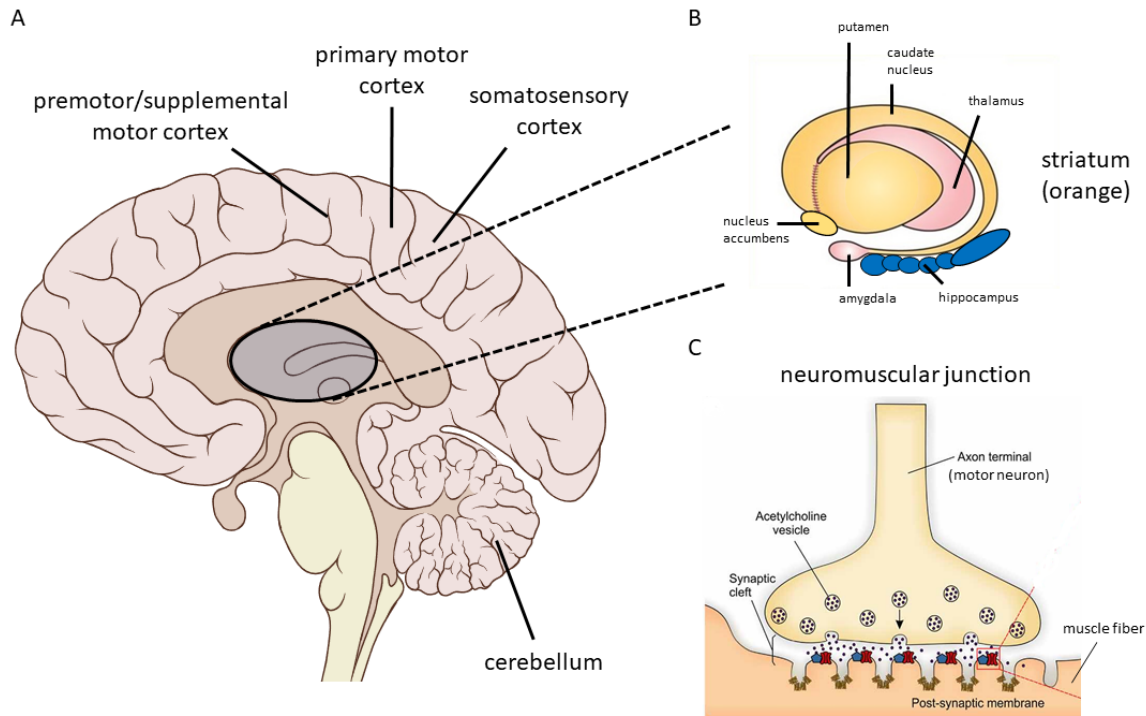
Through sequencing of total RNA, BK channels have been found to be expressed primarily in brain tissue, with only smooth muscle tissue (i.e., uterus, bladder, prostate and endometrium) surpassing brain tissue expression (Duff et al., 2015; Fagerberg et al., 2014). In mice, BK channels are expressed in brain regions associated with motor control including the cerebellum, striatum and motor/somatosensory cortex (Sausbier et al., 2005). Additionally, BK channels are found in the neuromuscular junction (NMJ) and skeletal

muscle (Tricarico et al., 1997; Vatanpour and Harvey, 1995) (Appendix 1). In regulating APs and neurotransmitter release, changes in BK channels across these body regions could be factors in causing the display of dyskinesia phenotypes associated with *KCNMA1* patients.

In the brain, the olivo-cerebellar circuit involves Purkinje neurons associated with regulation of motor timing and coordination (Welsh et al., 1995). Purkinje neurons with *KCNMA1* gene deletions show a decrease in excitability through lower frequency neuronal firing rates. This decrease in neuronal excitability is also associated with ataxia in *KCNMA1* KO (*Kcnma1*^{-/-}) mouse models (Chen et al., 2010). Another brain region involved in motor function, the striatum, is responsible for motor control through precision movements and motor learning processes (Rueda-Orozco and Robbe, 2015). BK channels are associated with regulating repolarization of the AP in striatal cholinergic interneurons. Though BK channels are associated with AHP regulation, only slow AHPs have been investigated in striatal neurons, associated with small conductance potassium (SK) channels (Bennett et al., 2000; Goldberg and Wilson, 2005; Wilson and Goldberg, 2006). The regulation of AP repolarization in striatal neurons could suggest involvement of BK channels in neuronal excitability, similar to *Kcnma1*-deleted Purkinje neurons. Next, BK channels in the somatosensory cortex, involved in processing sensory information, can block neuronal excitation. This is evident through pharmacological block of the channel increasing neuronal firing rates (Benhassine and Berger, 2009). There has also been recent evidence of BK channel association in synaptic plasticity of somatosensory neurons through negative feedback of intracellular-Ca²⁺-regulating N-methyl-D-aspartate (NMDA) receptors (Gómez et al., 2021). Finally, unlike these prominent areas of motor control and

movement coordination, there is a lack of literature on the roles of BK channels in the motor cortex, either on a cellular or behavioral level. However, the motor cortex is involved in neuronal pathways with parts of the striatum, somatosensory cortex and cerebellar vermis (responsible for posturing and locomotive control in the cerebellum) (Coffman et al., 2011; Künzle, 1975; Veinante and Deschenes, 2003). All of these brain regions associated with motor control express BK channels and could be factors in *KCNMA1* patient dyskinesia (Sausbier et al., 2005).

Figure 1.1. Expression of BK channels in brain regions associated with motor control, coordination and processing. (A) Sagittal slice of brain. Cerebellar Purkinje neurons are principle output neurons of the cerebellum that form projections along the olivo-cerebellar circuit which inhibit target cells of deep cerebellar nuclei (Fredette and Mugnaini, 1991). In the somatosensory cortex, dysfunction of the magnesium transporter *NIPA2* reduces BK channel function and in turn enhances neuronal excitability in somatosensory pyramidal neurons (Liu et al., 2019). (B) Striatum in relation to thalamus, amygdala and hippocampus locations. BK channel blockers broaden the AP width in the repolarizing phase while Ca^{2+} chelators do not (Bennett et al., 2000; Goldberg and Wilson, 2005). This suggests a colocalization of Ca^{2+} and BK channels in striatal neurons as BK channels are activated by Ca^{2+} (Goldberg and Wilson, 2005). (C) Neuromuscular junction (NMJ) with image modified from (Campanari et al., 2016). In the NMJ, BK channel blockers, such as iberiotoxin, decrease fast AHP amplitude, broaden the repolarizing phase and increase pre-synaptic release of ACh (Ford and Davis, 2014; Pattillo et al., 2001; Vatanpour and Harvey, 1995)



Along with motor control brain regions, the NMJ and skeletal muscles could be additional factors in dyskinesia phenotypes. NMJ is the synapse where peripheral motor neurons terminate at muscle fibers. BK channels are associated with regulation of acetylcholine (ACh) neurotransmitter release from the pre-synaptic terminals (Robitaille and Charlton, 1992; Vatanpour and Harvey, 1995). Observed in *Drosophila*, *Xenopus* and mouse NMJ's, BK channels also regulate repolarization and fast AHP phases of APs (Ford and Davis, 2014; Pattillo et al., 2001; Vatanpour and Harvey, 1995). Through this mechanism, increases in neuromuscular signaling could be associated with the phenotypes of tremor and ataxia in *Kcnma1*^{-/-} mice.

In skeletal muscles, BK channels show multiple distinct properties associated with channel transcript splice variants of varying current amplitude, Ca²⁺-sensitivity and drug response (Dinardo et al., 2012; Maqoud et al., 2017). These property differences have been observed between fast and slow-twitch muscle fibers of rats (Tricarico et al., 2005).

Additionally, BK channels are associated with regulating intracellular Ca^{2+} which drives proliferation of myoblasts in skeletal muscles. Myoblasts from humans with myotonic dystrophy 1, a disease characterized by muscle weakness and wasting, show fewer functional BK channels leading to alterations of intracellular Ca^{2+} levels. This results in increased myoblast proliferation with a decreased ability to differentiate into muscle-forming myotubes (Tajhya et al., 2016). In support of this, *Kenma1^{-/-}* rat models show muscle atrophy and decreased grip strength (He et al., 2021). This muscle weakness phenotype could confound interpreting presentations of dyskinesia in *KCNMA1* patients.

Region		Expression Level
Cerebral cortex	External granule cell layer (II)	+++
	External pyramidal cell layer (III)	+++
	Internal granule cell layer (IV)	+++
	Internal pyramidal cell layer (V)	+++
Striatum	Dorsal striatum (caudate/putamen)	++
	Nucleus accumbens	+++
Cerebellum	Cortical Purkinje cell layer	++++
	Deep cerebellar nuclei	++++
Pons and medulla (Olivo-cerebellar circuit)	Inferior/superior olivary complex	+
	Superior paraolivary nucleus	+
	Paraolivary nuclei	++
	Periolivary nuclei	+
Neuromuscular junction		Pharmacologic blockade of mouse nerve-muscle preparation abolishes BK channel currents (Vatanpour and Harvey, 1995)
Skeletal muscle		Single channel currents recordings of BK channels from skeletal muscle fibers of adult rats observed in (Tricarico et al., 1997)

Table 1.1. Expression of BK channels across movement- and motor-related areas of the central and peripheral nervous system. Table modified from immunofluorescent staining results of (Sausbier et al., 2005), excluding neuromuscular junction and skeletal muscle (descriptions in table). Expression classified as: +, few; ++, moderate, intermediate; +++, high; +++++, very high.

1.3. Rodent Models of Dyskinesia

Rodent models of dyskinesia provide a means validating genotype-phenotype associations, investigating of molecular mechanisms and treatment of disease. Baseline and paroxysmal motor dysfunction have been investigated in rodent models of varying dyskinesia types. First, Huntington's disease has been investigated in the context of mice with extended CAG repeats in the huntingtin (*HTT*) gene. These mice have a baseline tremor, ataxia and increase in stereotypic behaviors. However, HD mice do not show any phenotypes of paroxysms outside of their baseline dyskinesia (Mangiarini et al., 1996). This is similar to the exclusive baseline dyskinesia phenotypes seen in *Kcnma1*^{-/-} mice and serve as a useful comparison to paroxysmal dyskinesias (Meredith et al., 2004; Sausbier et al., 2004).

While Huntington's disease mouse models show baseline dyskinesia phenotypes, other models show paroxysmal dyskinesias. Mouse models of Ca²⁺ channelopathies display a range of both baseline and paroxysmal dyskinesia phenotypes that include dystonic (rigid, abnormal) posturing, choreiform (writhing) movements and tonic-clonic (rhythmic contraction) movements. These mouse models are also associated with absence seizure activity (Shirley et al., 2008). *Tottering* and *Rocker* mice have spontaneous mutations in the *CACNA1A* gene that encodes the α 1a subunit of P/Q-type calcium channels. Both mouse models have a baseline ataxia described by wide stance and unsteady gait. However, these mouse models have different dyskinesia characteristics. *Rocker* mice have a lower frequency of paroxysms for shorter durations than *Tottering* mice (Shirley et al., 2008). Both mouse models displayed dystonic trunk and limb flexion, though *Tottering* mice display more tonic-clonic movement of the hindlimbs (Fureman et al., 2002; Shirley et al.,

2008). To test for triggers of paroxysms, *Tottering* mice have been given injections of caffeine and ethanol and exposed to multiple environmental disturbances. Each one of these triggers results in an increase in paroxysms, similar to triggers of some PNKD types (Fureman et al., 2002; Garone et al., 2020; McGuire et al., 2018). The range of phenotypes from Ca²⁺ channelopathy mouse models demonstrates that a variety of dyskinesias can arise from mutations of a single channel gene. Also, Ca²⁺ channelopathies could be relevant to *KCNMA1*-linked channelopathy due to BK channels' Ca²⁺-dependent activation (Dworetzky et al., 1994; McCobb et al., 1995; Pallanck and Ganetzky, 1994).

Recently, proline-rich transmembrane protein 2 (*PRRT2*) has been identified as the cause of another paroxysmal dyskinesia in patients with autosomal dominant inheritance (Chen et al., 2011). Since then, mouse models of *PRRT2*-deficiency and KO have been developed to further investigate this dyskinesia. *PRRT2* KO mice show backwards locomotion, uncontrolled grooming and spontaneous dyskinetic movement of unknown origin (Michetti et al., 2017; Robertson et al., 2019). *PRRT2*-deficient mice show higher dyskinesia scoring upon optogenetic stimulation of the cerebellar vermis (Tan et al., 2018). However, the choreiform movements associated with scoring dyskinesia in both Ca²⁺ channelopathy and *PRRT2* mouse models do not resemble cataplexic/immobile nature of *KCNMA1* 'drop attacks' (Du et al., 2005; Heim et al., 2020; J. Heim, 2019; Miller et al., 2021; Shirley et al., 2008; Tan et al., 2018).

On the other hand, the *PNKD* gene, formerly known as MR1, has been associated with an autosomal dominant PNKD disorder (Lee et al., 2012; Rainier, 2004). The *PNKD* gene product is expressed in the striatum, cerebellum and spinal cords of mice. *PNKD* is expressed in both dopaminergic neurons projecting to the striatum as well as Purkinje cells

of the cerebellum. *PNKD* KO mice show no spontaneous paroxysms while mutant mice harboring patient mutations (*PNKD* mut-Tg) show spontaneous paroxysms of abnormal limb movement and excessive stereotypic movements upon stressful handling (Lee et al., 2012). Also, only *PNKD* mut-Tg show axial stiffness upon ethanol-induced paroxysms that more resemble ‘drop attack’ paroxysms in *KCNMA1* patients (Bailey et al., 2019; Lee et al., 2012). Both caffeine and ethanol injections resulted in higher levels of dopamine metabolites in the striatum associated with these paroxysms. This dysregulation of dopamine in *PNKD* mut-Tg mice suggests a role in striatum for motor dysfunction, though the cortical regions cannot be ruled out (Lee et al., 2012). As *PNKD* mut-Tg mice have paroxysmal dyskinesia trigger from stress, ethanol and caffeine, they more closely model *PNKD* compared to other models of dyskinesia.

However, evaluating rodent models of dyskinesia poses innate difficulties. First, differences in gait, weight-bearing and posturing make it difficult to relate phenotypes observed in rodent models to human patient phenotypes. For example, early symptoms of motor dysfunction in Huntington’s disease include involuntary orofacial and distal extremity movements (Roos, 2010). In a rodent model, these movements occur on a much smaller scale and can be hard to distinguish. Additionally, describing *KCNMA1* patient *PNKD* ‘drop attacks’ in rodent models could hold its own challenges. Immobility and rigidity of extremities may not present itself in a recognizable manner – quadrupedal rodents may not collapse like *KCNMA1* patients do during ‘drop attacks.’ Additionally, clinical reports of dyskinesia are often presented as case studies and can be limited to qualitative clinical observation of behavior as a diagnosis. This can lend itself to starting investigation of disease mechanisms in molecular and rodent models, but lacks quantitative

findings that can directly correlate with these models. This is most often the case when quantitative clinical diagnostics are invasive, such as muscle probing. Therefore, these difficulties in human-rodent model relations should be considered when interpreting genotype-phenotype relations.

Mouse Strain	Baseline Dyskinesia	Paroxysmal Dyskinesia	Epilepsy	Source
<i>Kcnma1</i> ^{-/-}	Ataxia, tremor	No	No	(Meredith et al., 2004; Sausbier et al., 2004)
R6 (<i>HTT</i>)	Ataxia, tremor, chorea	No	No	(Mangiarini et al., 1996)
Ca ²⁺ channelopathies (<i>Cacna1a</i> , <i>Cacnb4</i> , <i>Cacng2</i>)	Ataxia	PxD	Absence	(Fureman et al., 2002; Khan et al., 2004; Khan and Jinnah, 2002; Shirley et al., 2008)
<i>PRRT2</i> deficient/KO	No	PKD	No	(Michetti et al., 2017; Tan et al., 2018)
<i>PNKD</i> mut-Tg	No	PNKD	No	(Lee et al., 2012)

Table 1.2. Comparative rodent models of dyskinesia. Rodent models associated with baseline and paroxysmal forms of dyskinesia based on prior literature available of motor and behavioral assessments. PxD = paroxysmal dyskinesia (unknown trigger); PKD = paroxysmal kinesigenic dyskinesia; PNKD = paroxysmal non-kinesigenic dyskinesia.

1.4. Phenotypes of KCNMA1 Patient Variants in Cellular Expression Systems and Rodent Models

About half of *KCNMA1* variants are divided into characterizations of gain-of-function (GOF) and lose-of-function (LOF) properties based on changes in BK channel function in cellular heterologous expression systems (Bailey et al., 2019; Miller et al.,

2021). *KCNMA1* GOF variants are characterized by an increase in BK channel current magnitude or duration, whereas LOF variants impose a decrease in current magnitude or duration. Other variants are defined as either benign, showing no significant change in BK channel current magnitude or duration, or of unknown significance (Miller et al., 2021). In heterologous expression systems, both D434G and N999S mutations speeds BK channel opening and slows closing, as well as opening occurring at more hyperpolarizing voltages. These functional changes have thus categorized both variants as GOF (Diez-Sampedro et al., 2006; Du et al., 2005; Li et al., 2018; Moldenhauer et al., 2020; Wang et al., 2009; Yang et al., 2010).

D434G mutations show activation at more hyperpolarizing voltages at given Ca^{2+} concentrations with smaller changes in voltage-sensitive activation at increasingly saturated concentrations of Ca^{2+} (Du et al., 2005; Wang et al., 2009; Yang et al., 2010). This indicates that BK channels with the D434G mutation have increased Ca^{2+} -sensitivity, but not as much increased voltage-sensitivity. On the other hand, N999S mutations also show activation at more hyperpolarizing voltages, but with little difference in $V_{1/2}$ (test voltage at half the maximal conductance) in varying Ca^{2+} concentrations (Li et al., 2018; Moldenhauer et al., 2020). This indicates that unlike BK channels with D434G mutations, N999S mutant channels have an increased voltage sensitivity independent of Ca^{2+} gating. Compared to D434G mutant channels, N999S mutant channels activate faster and at more hyperpolarizing voltages. This results in an increased current magnitude in evoked APs of N999S mutant channels over D434G, suggesting that the N999S variant has stronger GOF than D434G (Moldenhauer et al., 2020).

Though *KCNMA1* variants are associated with changes in BK channel properties

and PNKD in patient harboring these variants, there is lack of family pedigrees and evidence in existing literature that these variants cause the PNKD observed in patients. Along with N999S and D434G variants, two LOF variants are associated with ataxia, tremor, axial hypotonia and generalized epilepsy. These LOF variants, R1097H and H444Q, are observed to display PNKD in one patient of each variant type (Bailey et al., 2019; Miller et al., 2021). Additionally, because the absence of BK channels implicitly abolishes BK channel currents, *Kcnma1*^{-/-} mice can be considered the most severe LOF model. *Kcnma1*^{-/-} mice show shorter strides than their WT controls in paw-print gait analysis, implicating a pervasive phenotype of ataxia. These mice also showed impaired performance on motor assays including walking beam, rotarod and hanging wire assays, which test balance, locomotor coordination and grip respectively (Meredith et al., 2004; Sausbier et al., 2004). These *Kcnma1*^{-/-} mouse phenotypes are associated with decreases in neuronal excitability as well. This occurs in KO models of BK channel-expressing cerebellar Purkinje neurons, which are known for locomotor regulation (Chen et al., 2010).

Bridging the gap between these cellular/physiologic roles of BK channels and patient symptoms is necessary to the mechanistic understanding of *KCNMA1*-linked channelopathy. Based on prior studies it is known that: (a) N999S and D434G variants are clinically associated with PNKD and show GOF effects on BK channel property in cellular heterologous expression systems, (b) R1097H and H444Q LOF variants also show clinical association with PNKD and (c) *Kcnma1*^{-/-} mice, considered to be a severe LOF model, show baseline ataxic dyskinesia that are associated with decreases in excitability of locomotor- and coordination-regulatory cerebellar Purkinje neurons. Thus, it is hypothesized that *KCNMA1* variants will cause dyskinesia phenotypes in mice. Validation

of patient phenotypes in these *KCNMA1*-linked channelopathy mouse models provides a means for further investigation into causal mechanisms of patient PNKD. This hypothesis will be tested through the following specific aims.

CHAPTER 2: SPECIFIC AIMS AND RATIONALE

In order to test the hypothesis that KCNMA1 variants cause dyskinesia in mice, motor assays are necessary to evaluate *Kcnma1*^{N999S/WT} and *Kcnma1*^{D434G/WT} phenotypes. The hypothesis would be supported by these mice exhibiting motor abnormalities through dyskinesia paroxysms like *KCNMA1* PNKD patients. However, *Kcnma1*^{N999S/WT} and *Kcnma1*^{D434G/WT} mice do not exhibit any apparent dyskinesia paroxysms or baseline motor abnormalities upon everyday caretaking observation. This is opposed to *Kcnma1*^{-/-} mice, who show an apparent tremor upon handling and noticeable hyperactivity within their home cage. Additionally, other rodent models of dyskinesia have been evaluated with elicited and spontaneous motor assays to characterize more specific aspects of motor phenotypes, including *Kcnma1*^{-/-} mice. Performance deficits and motor abnormalities in these assays can provide further insight to the quality and severity of motor phenotypes in these dyskinesia models. As such, it would be expected that *Kcnma1*^{N999S/WT} and *Kcnma1*^{D434G/WT} mice would show similar motor assay abnormalities, as outlined in each specific aims section.

The hypothesis is tested through a series of spontaneous and non-spontaneous motor assays on CRISPR-generated mice harboring N999S (*Kcnma1*^{N999S/WT}) and D434G (*Kcnma1*^{D434G/WT}) GOF mutations. As mice harboring patient LOF variants are not currently available at the time of this study, *Kcnma1*^{-/-} mice represent severe LOF baseline dyskinesia, as well as positive controls of assays with prior results from *Kcnma1*^{-/-} literature. All WT littermates are used as negative controls to establish normal motor performance, along with heterozygous *Kcnma1*^{+/-} mice as they have shown no significant performance deficits or other apparent abnormal phenotypes.

2.1. Elicited Motor Function

*The goal of this specific aims is to evaluate *Kcnma1* mutant and *Kcnma1*^{-/-} motor function and dyskinesia through assessing performance of elicited tasks. The hanging wire and rotarod assays test grip and locomotor coordination respectively through measuring fall latency times of mice. Furthermore, the rotarod assay can also assess motor learning in repeated measures where mice are trialed across multiple days. Both are considered to be non-spontaneous motor assays as grip and locomotor behaviors are forced by the investigator during observation. In this manner, mice are tested on baseline phenotypes and experience an acute stress of the assay, which could elicit dyskinesia paroxysms based on stress as a trigger of PNKD (McGuire et al., 2018).*

In mouse models of dyskinesia, Ca²⁺ channelopathy lethargic and stargazer mouse models of paroxysmal dyskinesia both show lower fall latency times compared to their WT littermates in hanging wire and rotarod assays (Khan et al., 2004; Khan and Jinnah, 2002). Also, *PRRT2*-deficient and KO mice show similar lower latency times during rotarod assays as well (Pan et al., 2020; Tan et al., 2018). Finally, mice harboring the D434G mutation have been recently tested on rotarod, in which lower latency times were seen in both heterozygous and homozygous mutant mice (Dong et al., 2021). Though none of these mouse models explicitly show symptoms of *KCNMA1*-like ‘drop attacks’, they show paroxysmal dyskinesia phenotypes that are associated with performance deficits in elicited motor assays.

Similar to these mouse models, *Kcnma1*^{-/-} mice also show lower fall latency times in both assays due to their ataxic phenotype (Meredith et al., 2004; Sausbier et al., 2004).

Because of this, *Kcnma1*^{-/-} mice are used as positive controls and a LOF baseline dyskinesia comparison on elicited motor assays. Based on prior results from *Kcnma1*^{-/-} mice and dyskinesia mouse models, *Kcnma1*^{N999S/WT}, *Kcnma1*^{D434G/WT} and *Kcnma1*^{-/-} mice are expected to show shorter fall latency times than their WT controls throughout all seven days of trailing. The elicited motor assays will likely not delineate baseline and paroxysmal dyskinesia between *Kcnma1* mutant groups and *Kcnma1*^{-/-} groups. This is because motor abnormalities are expected to be presented as shorter fall latency times and/or impaired motor learning in all groups regardless of dyskinesia type. Though motor learning is not analyzed in prior literature of paroxysmal dyskinesia models, paroxysms could disrupt and thus impair learning in *Kcnma1* mutant groups.

2.2. Spontaneous Motor Function

The goal of this specific aims is to evaluate Kcnma1 mutant and Kcnma1^{-/-} motor function and dyskinesia through assessing spontaneous activity and behavior. CatWalk gait analysis, free-running wheel activity and restraint-induced dyskinesia analysis are all assays that are considered to be analysis of spontaneous activity, as no behavior is forced by the investigator during observation. The CatWalk system has been used to assess gait disturbances in HD rat and mouse models. Both models show higher hindlimb swing speeds (the speed at which a paw moves while not in contact with the glass) with the mouse model eventually developing higher forelimb swing speed at a later age (Casaca-Carreira et al., 2015; Timotius et al., 2019). In rat HD models, this gait abnormality was shown to be associated with baseline choreiform dyskinesia through observational scoring (Casaca-Carreira et al., 2015; McGuire et al., 2018). Also, using a treadmill style gait analysis

(DigiGait), *PRRT2* KO mice show both a shorter stride duration and stride length, similar to CatWalk results of HD models (Casaca-Carreira et al., 2015; Robertson et al., 2019; Timotius et al., 2019).

As with HD mouse models, prior CatWalk gait analysis of *Kcnma1*^{-/-} mice has also shown shorter stride length than both *Kcnma1*^{-/+} and *Kcnma1*^{+/+} controls, and thus are used as a positive control and LOF baseline dyskinesia comparison (Typlt et al., 2013). This also means baseline and paroxysmal dyskinesias may have similar presentations from gait analysis. Because of this, *Kcnma1*^{N999S/WT}, *Kcnma1*^{D434G/WT} and *Kcnma1*^{-/-} mice are expected to show baseline gait abnormalities in parameters related to stride length, swing speed, print area and step patterns. Differences in forelimb and hindlimb parameters between groups may provide delineations between *Kcnma1* mutant groups and *Kcnma1*^{-/-} groups, as ataxic phenotypes are more often observed as hindlimb-specific gait disturbances in *Kcnma1*^{-/-} mice (Chen et al., 2010; Sausbier et al., 2004; Typlt et al., 2013). A ‘drop attack’-like paroxysm in *Kcnma1* mutant mice would present as immobility of all four limbs. Thus, gait disturbances would be expected to happen in both forelimbs and hindlimbs, unlike ataxic gaits in mice.

Free-running wheel activity has also been used in assessing early motor deficits in HD mouse models. Decreases in wheel activity during the 12-hour dark active phase were seen at ages as early as 4.5-5.5 weeks, with progressively lower activity in both light and dark phases up until 6 months. These deficits in wheel activity also coincided with lower fall latency times on rotarod (Hickey et al., 2005; Hickey et al., 2008). In another study, HD mice showed wheel activity deficits in run distance and duration within the first week of analysis when a rotarod assay showed no significant difference in fall latency times

(Mandillo et al., 2014). Additionally, because stress triggers paroxysms in *KCNMA1* PNKD patients, a shorter 48-hour analysis of wheel activity can additionally provide stresses of a novel environment. Based on prior HD mouse models and novel environment stresses, *Kcnmal*^{N999S/WT}, *Kcnmal*^{D434G/WT} and *Kcnmal*^{-/-} mice are expected to show decreased wheel activity in run distance/speed and duration. It may be difficult to delineate baseline and paroxysmal dyskinesia phenotypes between *Kcnmal* mutant groups and *Kcnmal*^{-/-} groups. Baseline ataxic dyskinesia of *Kcnmal*^{-/-} mice may disturb their gait enough to slow them on the wheels. On the other hand, ‘drop attack’-like paroxysms would present as pausing during running. This could result in lower run distance or average speed, but with a higher frequency of gaps in activity.

Finally, *KCNMA1* PNKD patients are reported to experience ‘drop attacks’ from stress triggers (Garone et al., 2020; Heim et al., 2020; Keros et al., 2021; McGuire et al., 2018; Wang et al., 2017). As such, spontaneous activity is observed following an acute stress via hand restraint which may elicit ‘drop attack’-like paroxysms in *Kcnmal* mutant mice. Though each of the prior assays has their own compliment of stress (novel environments of spontaneous assays and elicited behavior/handling of non-spontaneous assays), none of these assays provide direct observational analysis of behavior following a calibrated stressor. To give further support that expected outcomes of each one of these assays provides evidence of a ‘drop attack’-like phenotype in mice, the presence of any dyskinetic movements and paroxysms must be directly scored.

From other variations of dyskinesia scoring, Ca²⁺ channelopathy mice show higher scores, displaying severe paroxysms in choreiform movements and dystonic posturing, along with tonic-clonic movements. Scoring of these mice were done through various

modifications of a systematic method of measuring rodent stereotypic behavior and was performed on multiple Ca^{2+} channelopathy mouse models (Kelley, 1998; Khan et al., 2004; Khan and Jinnah, 2002; Shirley et al., 2008). Tottering mice were scored based on stress triggers where mice had the highest percentage of paroxysms during restraint (along with cage transport) (Fureman et al., 2002). *PNKD* mut-Tg mouse models showed dyskinesia paroxysms during stressful handling and upon observation in a beaker after vehicle control saline I.P. injections. Though the beaker creates a novel and further stressful constrained environment, controlled acute restraint was not performed as a stressor (Lee et al., 2012). An acute restraint provides a more well-defined mode of stress-induction than just “stressful handling”. Thus, dyskinesia scoring of *Kcnma1* mutant and *Kcnma1*^{-/-} mice occurs after controlled acute hand restraint followed by placement of mice into a beaker for additional stress of a small environment.

Based on prior observation of stress triggers inducing paroxysms in dyskinesia mouse models, *Kcnma1*^{N999S/WT}, *Kcnma1*^{D434G/WT} and *Kcnma1*^{-/-} mice are expected to show higher scores in abnormal movement categories. Delineation of baseline and paroxysmal dyskinesia phenotypes between *KCNMA1* mutations groups and *Kcnma1*^{-/-} groups could be possible in this assay. *Kcnma1*^{-/-} mice present baseline ataxia and tremors as opposed to paroxysms seen in patients harboring GOF variants (Meredith et al., 2004; Sausbier et al., 2004). This means that *Kcnma1*^{N999S/WT} and *Kcnma1*^{D434G/WT} mice would likely show bouts of dyskinetic movement compared to *Kcnma1*^{-/-} mice. Additionally, *KCNMA1* PNKD patients have paroxysms that resemble cataplexy, which could result in increased immobility in *Kcnma1* mutant groups (Miller et al., 2021).

CHAPTER 3: METHODOLOGY

3.1. Mice

All animal procedures and experiments were conducted in accordance with University of Maryland, Baltimore School of Medicine guidelines and protocols with approval from the Institutional Animal Care and Use Committee. 2- to 3-month-old mice are used in all experiments for *Kcnma1*^{N999S/WT} and *Kcnma1*^{D434G/WT} cohorts. Litters from these cohorts were generally healthy and produced in expected Mendelian ratios. 2- to 8-month-old mice are used for *Kcnma1*^{-/-} cohorts due to decreased breeding efficacy and difficulties with Mendelian ratios in litters (Meredith et al., 2004). Both male and female mice were used in all experimental cohorts. All experiments were performed blinded to genotype of the mice and data was analyzed blinded.

3.2. Hanging Wire

Mice are acclimated to the testing environment in their normal housing cages for one hour prior to testing. Mice body weights are measured prior to the start of testing. Three consecutive trials are then performed in one day. At the start of each trial, mice are placed right-side-up on a standard housing lid with parallel metal bars. The lid is gently shaken three times to provoke the mice to grasp the bars, then slowly inverted upside-down so the mice are hanging. The fall latency time is measured via stopwatch, which begins counting at the start of lid inversion. Trial duration lasts for a maximum of 120 seconds. Mice are given at most a 10 second inter-trial interval after falling. If mice reach the 120 second trial limit, the lid is once again inverted to right-side-up and the mice are given a 10 second inter-trial interval before beginning the next trial. Statistical analysis is performed on

Kcnma1^{-/-} cohorts using One-way ANOVA with Welch's correction and Dunnett's T3 post-hoc test for multiple comparisons. Unpaired t-test with Welch's correction is used for *Kcnma1*^{N999S/WT} and *Kcnma1*^{D434G/WT} cohorts.

3.3. Rotarod

Mice are acclimated to the testing environment in their normal housing cages for one hour prior to testing. Mice are trialed 3 times a day for 7 consecutive days. On day 1, mice body weight is measured and then randomly placed in one of the five lanes of the rotarod device (IITC Life Science Inc. Rat Mouse Rotarod, provided by Dr. Todd Gould, PhD). After placement, mice are given 30 seconds prior to the start of day 1/trial 1 to acclimate to the beam. Mice are allowed to fall off and be placed back on the beam a maximum of two times. Any more than two falls prior to day 1/trial 1 or any one fall prior to any other trial is recorded as a fall latency time of 0 seconds. On day 7, mice body weight is measured once again. The rotarod device accelerates from 4 to 40rpm of the course of 5 minutes for each trial. Mice are given a 2-minute inter-trial interval. A "fall" is measured as the mice no longer maintaining an upright position on the beam, regardless of the mice truly falling off the beam. This is because on preliminary trialing mice were often able to hold onto the beam to avoid falling, which in turn no longer assesses locomotor coordination. All trials are video recorded and fall latency times are measured from each recording. The three trials of each day are averaged together for each mouse, then individual mice of each genotype are averaged together for each day. Statistical analysis is performed using Two-way ANOVA with Geisser-Greenhouse correction and Bonferroni's post-hoc test for multiple comparisons for all cohorts.

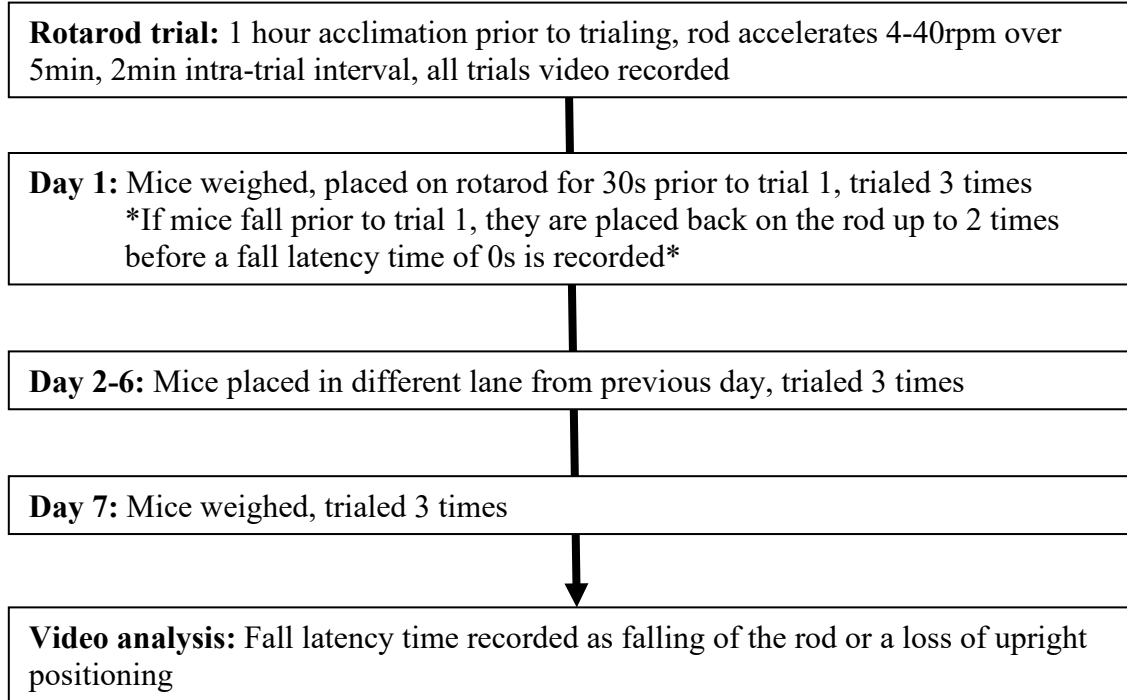


Table 1.3. Flow-chart of rotarod assay procedural timeline.

3.4. Gait Analysis (CatWalk XT)

The CatWalk XT system (Noldus Information Technology, provided by Dr. Junfang Wu, PhD) consists of a long glass plate that is illuminated internally by a green light. In a dark room, mice are placed on the glass and allowed to freely walk from one end to the other. Paw prints are detected by a high-speed camera positioned under the glass. Before placing the mice on the glass, mice are placed on a warm damp cloth to aid in paw illumination and software detection with minimal effect on gait. Mice are given as much time required to capture three runs across the camera's field of view, with compliant runs consisting of a 60% or less variability. CatWalk XT 10.6 software is used to capture recordings and analyze data. Because 174 gait parameters are captured and analyzed, parameters are selected based on preliminary trials of *Kcnma1*^{N999S/WT}, *Kcnma1*^{D434G/WT}

and *Kcnma1*^{-/-} mice, and prior gait analysis of Huntington's disease mouse models (Casaca-Carreira et al., 2015; Typlt et al., 2013). Statistical analysis is performed on *Kcnma1*^{-/-} cohorts using One-way ANOVA with Welch's correction and Dunnett's T3 post-hoc test for multiple comparisons. Unpaired t-test with Welch's correction is used for *Kcnma1*^{N999S/WT} and *Kcnma1*^{D434G/WT} cohorts.

3.5. Free-running Wheel Activity

Mice are singly housed in cages with running wheels (Coulbourn Instruments) on a standard 12:12-hour light-dark cycle for 48 hours with ad-libitum access to food and water. Mice health checks, room temperature and humidity monitoring are performed daily. Free-running wheel activity is measured via magnetic switches and recorded using ClockLab software (Actimetrics). Individual mice wheel rotation counts are then quantified in 1-minute bins in ClockLab software running in Matlab v6.1 (Mathworks). The following parameters are calculated for activity during the 12-hour dark phase: total wheel rotation count, average speed, average maximum speed, average number of run events (defined as consecutive 1-minute bins over 30rpm), average run duration, average maximum run duration, average run wheel rotation count, average number of activity gaps (defined as consecutive 1-minute bins of 0rpm), average activity gap duration and average maximum activity gap duration. These parameters are selected based on a modified method of analysis in HD mouse models (Mandillo et al., 2014). Analysis is performed using a self-made Python script. Statistical analysis is performed on *Kcnma1*^{-/-} cohorts using One-way ANOVA with Welch's correction and Dunnett's T3 post-hoc test for multiple comparisons. Unpaired t-test with Welch's correction is used for *Kcnma1*^{N999S/WT} and

Kcnmal^{D434G/WT} cohorts.

3.6. Restraint-induced Dyskinesia Analysis

Mice are restrained by hand by an experienced handler. This is done by clasping the loose skin of the dorsal cervical aspect with the index finger and thumb, and the tail with the pinky finger so that that dorsal side lay flat against the palm of the hand in a vertical upright position. This restraint lasts for 2.5 minutes. Afterwards, the tail is released by the pinky and the mice are restrained for another 2.5 minutes. The total restraint time lasts for 5 minutes Mice are then placed in a transparent 1000ml beaker and video-recorded for 5 minutes. Mice scoring is based on stereotypic (grooming, rearing, sniffing) and abnormal criteria (immobility time, circling/hyperactivity, twisting/choreiform movement, tonic-clonic movement, flatten dystonic posturing, tremoring, listing and falling). Grooming, twisting/choreiform movement, tonic-clonic movement, flatten dystonic posturing, listing and falling are scored in 30 second bins as either 0 (no occurrence of behavior) or 1 (behavior observed). Scores for criteria scored in 30 second bins are then totaled. Circling/hyperactivity and tremoring is scored as either a 0 or 1 for the full duration of the 5-minute recording. Rearing behavior is defined as both forelimb paws touching the sides of the beaker (Appendix Figure 2) and is counted as the total number of rears for the full duration of the recording. Grooming is defined as any stereotypical licking of the front paws or body while reared on both hindlimbs (Appendix Figure 2). Immobility is defined as the lack of head, body and limb movement with all four paws touching the ground (Appendix Figure 2). Immobility is continually timed at the start and stop of immobility using a stopwatch for the full duration of the recording. Behavioral scoring parameters are

selected based on preliminary trials of *Kcnma1*^{N999S/WT}, *Kcnma1*^{D434G/WT} and *Kcnma1*^{-/-} mice, modified stereotypic behavioral scoring (Kelley, 1998) and prior scoring of various dyskinesia mouse models (Khan et al., 2004; Khan and Jinnah, 2002; Sebastianutto et al., 2016; Shirley et al., 2008). Statistical analysis is performed on *Kcnma1*^{-/-} cohorts using One-way ANOVA with Welch's correction and Dunnett's T3 post-hoc test for multiple comparisons. Unpaired t-test with Welch's correction is used for *Kcnma1*^{N999S/WT} and *Kcnma1*^{D434G/WT} cohorts.

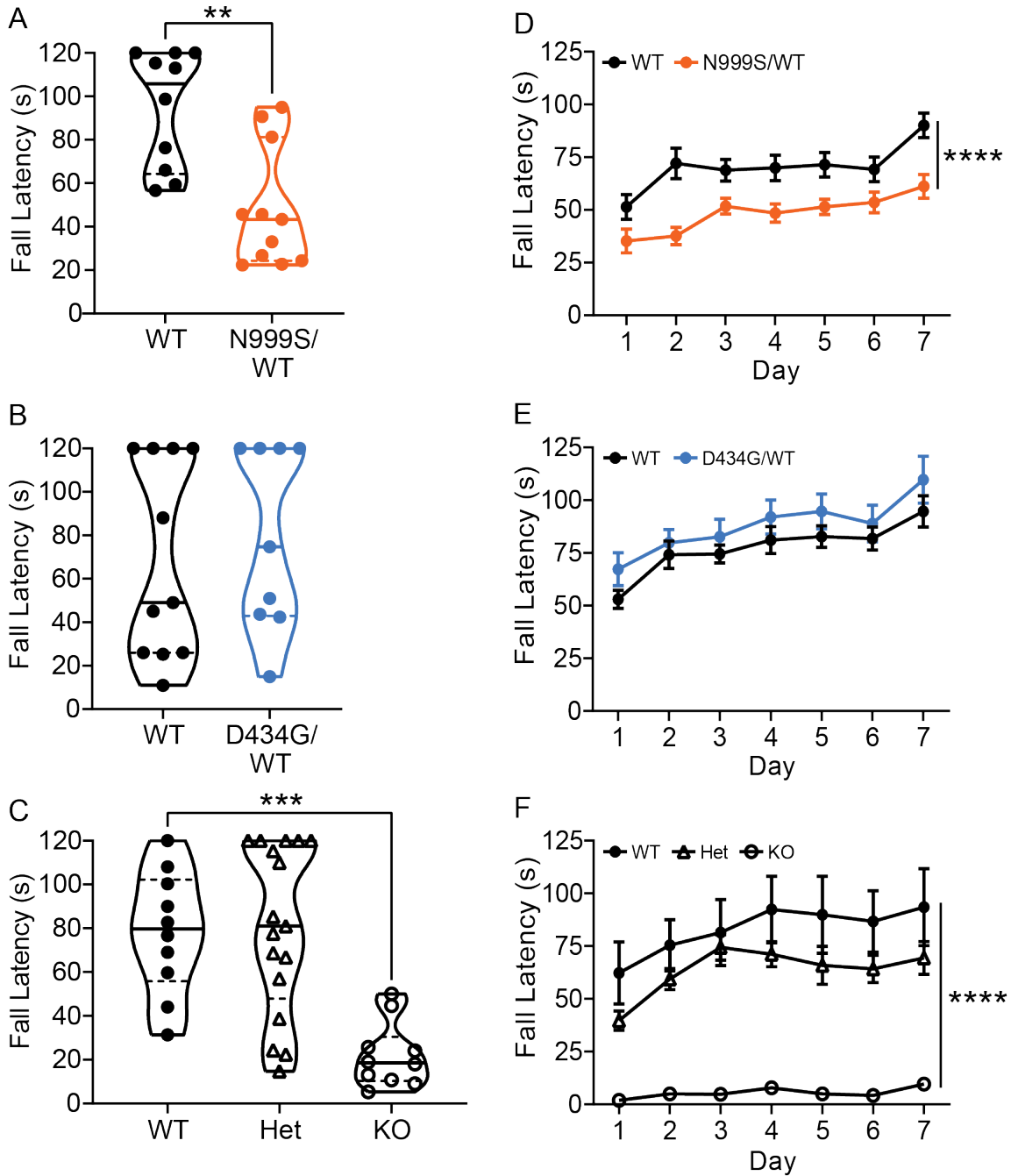
CHAPTER 4: RESULTS

4.1. *Kcnma1*^{N999S/WT} and *Kcnma1*^{-/-} Show Elicited Motor Impairment

To test the hypothesis that *KCNMA1* variants cause dyskinesia phenotypes in mice, a hanging wire and rotarod assay were performed. In the hanging wire assay, mice exhibiting *KCNMA1* patient-like ‘drop attacks’ would be expected to show shorter fall latency times due to hypotonia from dyskinesia paroxysms inhibiting grip. The baseline dyskinesia phenotypes of *Kcnma1*^{-/-} mice are also expected to shorten fall latency times, as seen in prior studies. The unsteady movement from tremors would be expected to also inhibit grip.

From the data, *Kcnma1*^{N999S/WT} mice show shorter fall latency times, with no mouse reaching the 120s threshold (Figure 4.1A). On the other hand, *Kcnma1*^{D434G/WT} mice did not show any significant difference in fall latency times compared to WT controls, with four *Kcnma1*^{WT/D434G} mice and four WT controls each reaching the 120s threshold across all three trials (Figure 4.1B). As expected, *Kcnma1*^{-/-} mice show shorter fall latency times compared to WT controls on the hanging wire assay, while *Kcnma1*^{-/+} mice show no significant difference (Figure 4.1C). Where most normal mice have fall latency times upwards of several minutes (Crawley, 2000), no individual *Kcnma1*^{-/-} mouse had a mean latency time above 60 seconds, compared to *Kcnma1*^{+/+} mice with mean latency times ranging from 31.33 to the 120 second trial limit. These results indicate that both *Kcnma1*^{N999S/WT} and *Kcnma1*^{-/-} mice have impaired grip, with *Kcnma1*^{-/-} mice showing a more severe impairment compared to *Kcnma1*^{N999S/WT} mice (unpaired t-test with Welch’s correction ; p=0.0148).

Figure 4.1. *Kcnmal*^{N999S/WT} and *Kcnmal*^{-/-} mice show lower fall latency times during elicited motor assays. (A-C) Fall latency times on hanging wire assay. (A) Unpaired t-test with Welch's correction show lower fall latency times in *Kcnmal*^{N999S/WT} mice (p=0.0010; n=10, *Kcnmal*^{WT/WT}; n=11, *Kcnmal*^{N999S/WT}). (B) Unpaired t-test with Welch's correction show no significant difference in fall latency times of *Kcnmal*^{D434G/WT} mice (p=0.6090; n=11, *Kcnmal*^{WT/WT}; n=9, *Kcnmal*^{D434G/WT}). (C) One-way ANOVA with Welch's correction shows lower fall latency times in *Kcnmal*^{-/-} mice (p<0.0001 main effect). Multiple comparisons from Dunnett's T3 post-hoc test shows significant difference in *Kcnmal*^{-/-} mice compared to *Kcnmal*^{+/+} mice (p=0.0093), while *Kcnmal*^{-/+} mice show no significant difference to *Kcnmal*^{+/+} mice (p=0.9982) (n=10, *Kcnmal*^{+/+}; n=17, *Kcnmal*^{-/+}; n=10, *Kcnmal*^{-/-}). (D-H) Fall latency times for rotarod assay. Two-way repeated measures ANOVA with Geisser-Greenhouse correction performed on all cohorts. (D) *Kcnmal*^{N999S/WT} mice show lower fall latency times (p<0.0001 main effect; n=12, *Kcnmal*^{WT/WT}; n=11, *Kcnmal*^{N999S/WT}). (E) *Kcnmal*^{D434G/WT} mice show no significant difference in fall latency times (p=0.1858 main effect; n=17, *Kcnmal*^{WT/WT}; n=13, *Kcnmal*^{D434G/WT}). (F) *Kcnmal*^{-/-} mice show lower fall latency times (p<0.0001 main effect). Multiple comparisons from Bonferroni's post-hoc test shows significant difference in *Kcnmal*^{-/-} mice compared to *Kcnmal*^{+/+} mice (lowest p=0.0056 and highest p=0.0277 from 7 days), while *Kcnmal*^{-/+} mice show no significant difference to *Kcnmal*^{+/+} mice (lowest p=0.5801 and highest p>0.9999 from 7 days) (n=6, *Kcnmal*^{+/+}; n=12, *Kcnmal*^{-/+}; n=6, *Kcnmal*^{-/-}).



With the rotarod assay, *Kcnmal* mutant mice are expected to have shorter fall latency times from *KCNMA1* ‘drop attack’-like dyskinesia paroxysms. Hypotonia and immobility during paroxysms would inhibit locomotor function during the rotarod task and thus lower latency times. This could in turn inhibit motor learning as well with paroxysms

disrupting learning processes. *Kcnma1*^{-/-} are also expected to have shorter latency times due to baseline ataxia and tremors inhibiting locomotor function. The association of these baseline dyskinesia phenotypes with cerebellar Purkinje neuronal firing inhibition are expected to also inhibit motor learning (Chen et al., 2010).

From the data, *Kcnma1*^{N999S/WT} mice show shorter fall latency times over the course of seven days compared to their WT controls (Figure 4.1D). However, *Kcnma1*^{N999S/WT} mice show no significant difference in motor learning throughout the seven days of testing. To quantitatively assess motor learning, a preliminary analysis of a linear regression fitted to the fall latency means of all seven days was performed. From this, *Kcnma1*^{N999S/WT} mice show no significant difference in fall latency (motor learning) slopes to WT controls ($R^2=0.6013$, *Kcnma1*^{WT/WT}; $R^2=0.8546$, *Kcnma1*^{N999S/WT}; $p=0.9421$). On the other hand, *Kcnma1*^{D434G/WT} mice did not show any difference in overall fall latency times over the course of seven days compared to their WT controls (Figure 4.1E). *Kcnma1*^{D434G/WT} mice also show no significant difference in motor learning throughout the seven days of testing. In the preliminary linear regression, *Kcnma1*^{D434G/WT} mice show no significant difference in motor learning slopes to WT controls ($R^2=0.8104$, *Kcnma1*^{WT/WT}; $R^2=0.8380$, *Kcnma1*^{D434G/WT}; $p=0.8496$). These findings indicate that, unlike *Kcnma1*^{D434G/WT} mice, *Kcnma1*^{N999S/WT} mice have impaired locomotor function in elicited motor assays. However, both groups show no indication of impaired motor learning.

As a comparison of baseline dyskinesias, *Kcnma1*^{-/-} mice show shorter fall latency times over the course of seven days compared to WT controls, while *Kcnma1*^{-/+} mice show no significant difference (Figure 4.1F). No individual *Kcnma1*^{-/-} mouse had a mean latency time over 30 seconds on any given day, compared to WT controls ranging from 30.33 to

148.0 seconds. In addition, *Kcnma1*^{-/-} mice show lower motor learning slopes in the preliminary linear regression than WT controls throughout the seven days of testing ($R^2=0.7416$, *Kcnma1*^{+/+}; $R^2=0.4486$, *Kcnma1*^{-/-}; $p=0.0142$). On the other hand, *Kcnma1*^{-/+} mice show no significant difference in motor learning slopes ($R^2=0.7416$, *Kcnma1*^{+/+}; $R^2=0.3628$, *Kcnma1*^{-/+}; $p=0.5939$). Additionally, *Kcnma1*^{N999S/WT}, *Kcnma1*^{D434G/WT}, *Kcnma1*^{-/+} mice and all WT controls show multiple days with higher trial 3 fall latency times than trial 1 (Figure 4.2D-F). This shows a trend of motor learning during the three trials of each day. However, this is not observed during any day of trialing for *Kcnma1*^{-/-} mice (Figure 4.2F). Also, compared to *Kcnma1*^{N999S/WT} mice, *Kcnma1*^{-/-} mice show a significantly lower main effect of latency times (Two-way repeated measures ANOVA with Geisser-Greenhouse correction; $p<0.0001$). Because of this, these data indicate that *Kcnma1*^{-/-} mice have a more severe locomotor deficit in elicited motor assays than *Kcnma1*^{N999S/WT} mice. However, neither of these assays are capable of making a distinction between a baseline and paroxysmal dyskinesia. Both *Kcnma1*^{N999S/WT} and *Kcnma1*^{-/-} mice show lower fall latency times on both assays. Though *Kcnma1*^{-/-} mice show impaired motor learning as opposed to *Kcnma1*^{N999S/WT} mice, this is not a conclusive delineation of paroxysms in *Kcnma1*^{N999S/WT} mice.

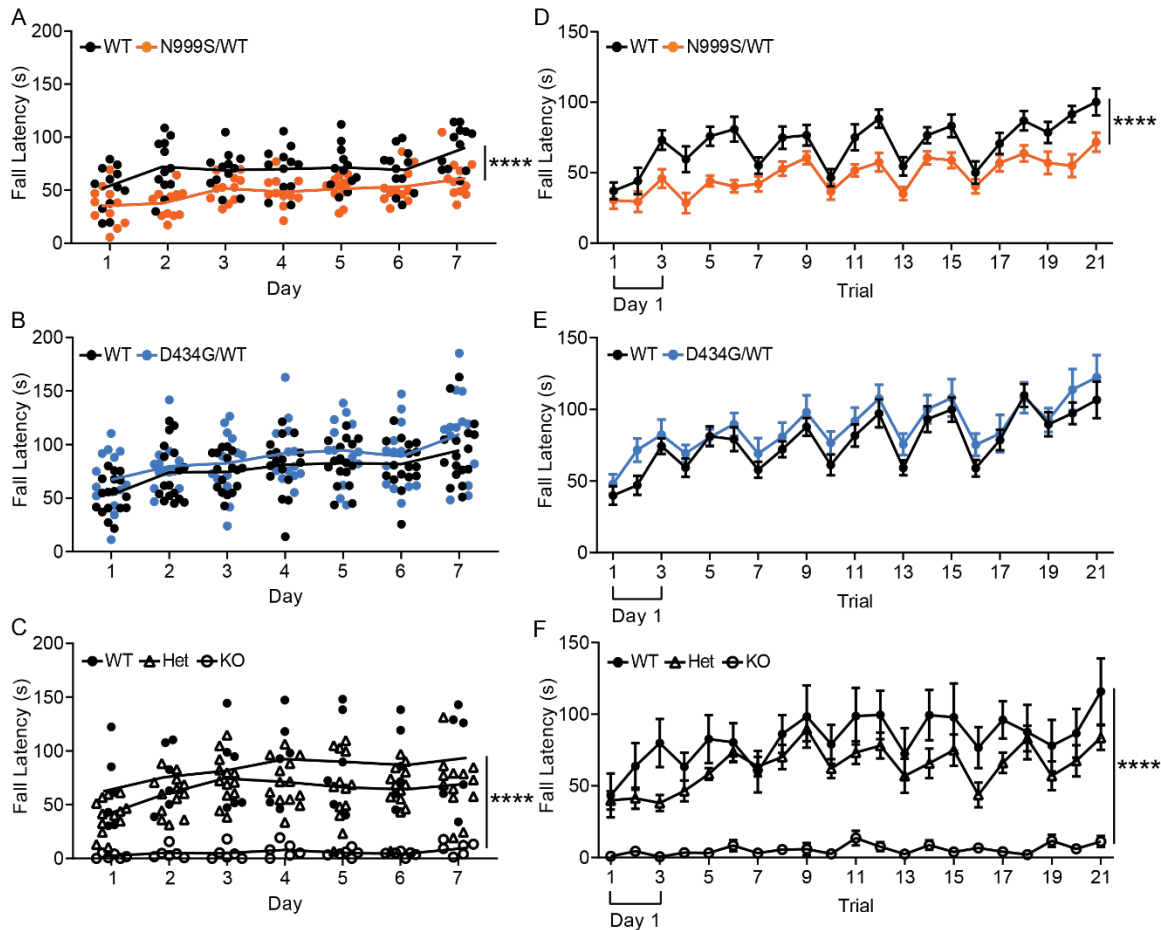


Figure 4.2. *Kcnma1*^{-/-} mice show motor learning deficits. Fall latency times for rotarod assays. (A-C) Interleaved scatter plot of individual animal trial means. (D-F) Means of each individual trial (three trials per day) plotted in succession as 21 trials. (A, D) Two-way repeated measures ANOVA with Geisser-Greenhouse correction shows lower latency times in *Kcnma1*^{N999S/WT} mice ($p < 0.0001$ main effect; $n = 12$, *Kcnma1*^{WT/WT}; $n = 11$, *Kcnma1*^{N999S/WT}). (B, E) Two-way repeated measures ANOVA with Geisser-Greenhouse correction shows no significant difference in latency times in *Kcnma1*^{D434G/WT} mice to WT controls ($p = 0.1858$ main effect; $n = 17$, *Kcnma1*^{WT/WT}; $n = 13$, *Kcnma1*^{D434G/WT}). (C, F) Two-way repeated measures ANOVA with Geisser-Greenhouse correction shows lower latency times in *Kcnma1*^{-/-} ($p < 0.0001$ main effect). Multiple comparisons from Bonferroni's post-hoc test shows significant difference in *Kcnma1*^{-/-} mice compared to *Kcnma1*^{+/+} mice (lowest $p = 0.0056$ and highest $p = 0.0277$ from 7 days), while *Kcnma1*^{-/+} mice show no significant difference in latency times to *Kcnma1*^{+/+} mice (lowest $p = 0.5801$ and highest $p > 0.9999$ from 7 days) ($n = 6$, *Kcnma1*^{+/+}; $n = 12$, *Kcnma1*^{-/+}; $n = 6$, *Kcnma1*^{-/-}).

4.2. $Kcnma1^{N999S/WT}$ and $Kcnma1^{-/-}$ Mice Show Unique Spontaneous Motor Impairment Suggestive of Dyskinesia

For CatWalk, if *KCNMA1* variants cause dyskinesia in mice, it would be expected that *Kcnma1* mutant mice would show gait disturbances in all four limbs. A *KCNMA1* patient-like ‘drop attack’ in mice would cause paroxysms in which there would be a lack of movement in all four limbs (Heim et al., 2020; J. Heim, 2019). This is opposed to *Kcnma1*^{-/-} mice which are expected to have gait disturbances in only the hindlimbs from baseline ataxic phenotypes (Typlt et al., 2013). These differences can provide a distinction between *Kcnma1* mutant groups and *Kcnma1*^{-/-} mice, unlike elicited motor assays.

Assessment of weight differences between experimental and control mice within groups was done prior to data analysis. In prior literature, *Kcnma1*^{-/-} mice did not show any difference in paw print area in Typlt et al., 2013, where *Kcnma1*^{-/-} mice in our data show differences in paw print area, contact area and intensity parameters (paw parameters). Because these parameters are all measures of the paw image alone (not movement), weight differences can affect the significance of these parameters. For example, it would be expected that heavier mice would record higher values in paw parameters as more contact is likely to be made with the glass. This is seen between our *Kcnma1*^{-/+} males (n=6) and females (n=4), where 18 of the 64 paw parameters show significant differences. Only 4 other parameters out of the total 174 analyzed show significant differences. This weight difference is not seen the prior study of *Kcnma1*^{-/-} mice, possibly due to a different genetic background (hybrid SV129/C57BL6) (Typlt et al., 2013) than our *Kcnma1*^{-/-} mice (C57BL6). Thus, because our *Kcnma1*^{-/-} mice weigh significantly less than *Kcnma1*^{+/+} mice, paw parameters have been excluded from CatWalk analysis (Appendix Figure 2).

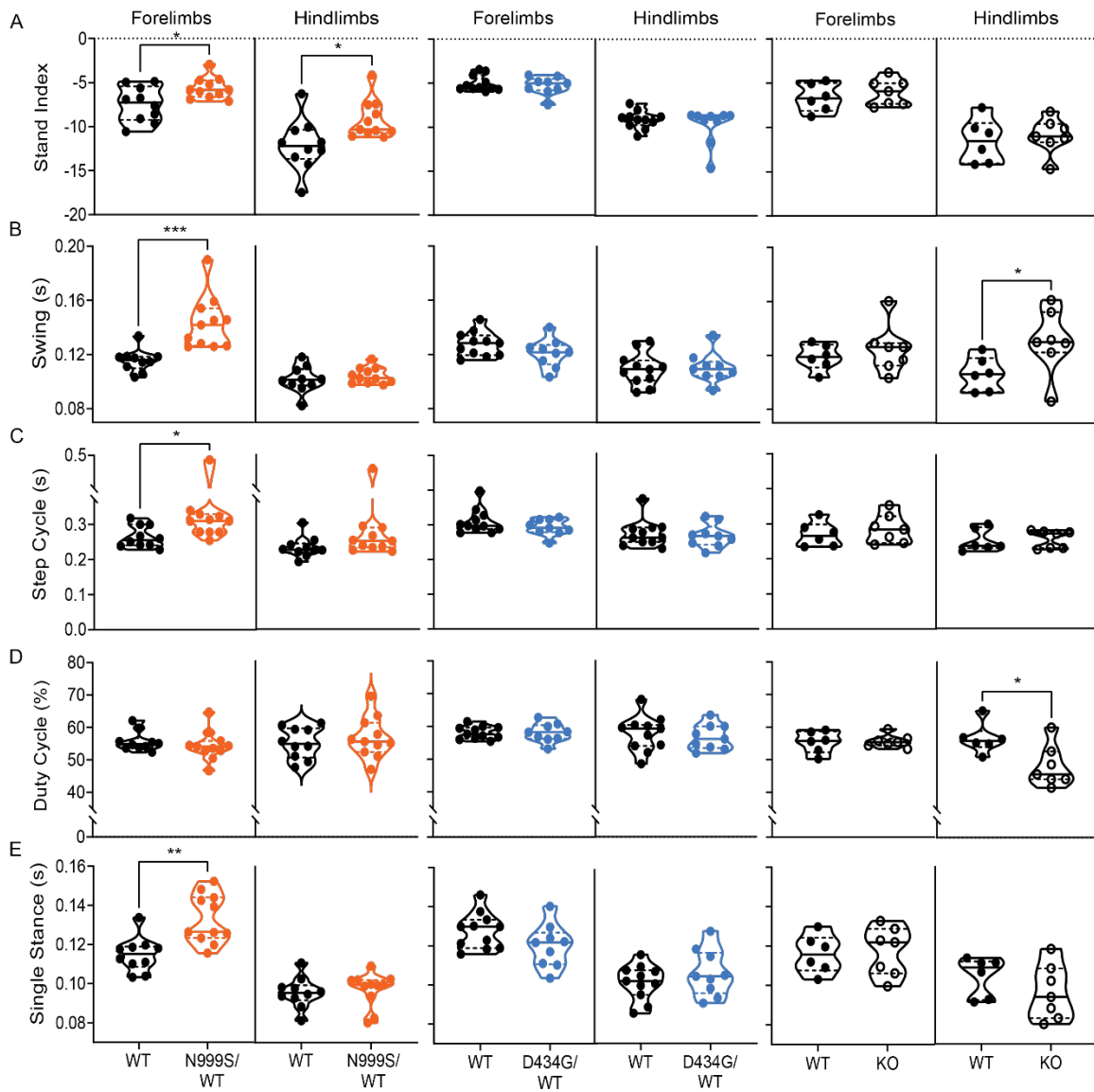
From gait analysis of all other parameters, *Kcnma1*^{-/-} mice show abnormalities in

parameters that indicate ataxia. *Kcnmal*^{-/-} mice have a higher swing duration of the hindlimbs, which is the duration that the paw is not contacting the plate between a contact termination and initiation (Figure 4.3C). Additionally, *Kcnmal*^{-/-} mice show a slower swing speed, which is the stride length over the swing duration (Appendix Table 3). The step cycle is the total duration of paw contact in addition to the swing duration, in which *Kcnmal*^{-/-} mice show no significant difference to WT controls (Figure 4.3D). However, *Kcnmal*^{-/-} mice show a lower duty cycle of the hindlimbs, which is the percent time of paw contact out of the step cycle (Figure 4.3E). This means that *Kcnmal*^{-/-} mice show longer swing and shorter paw contact duration, though the total of the two (the step cycle) shows no significant difference. *Kcnmal*^{-/-} mice show no significant difference in stand index, or the rate in which the paw loses contact with the glass (Figure 4.3A). And finally, *Kcnmal*^{-/-} mice show no significant difference in single stance, or the duration that a single forelimb or hindlimb paw makes contact while the other collateral paw does not (Figure 4.3F). Though *Kcnmal*^{-/-} mice do not show a significant difference in stride length, the longer swing duration, lower swing speed and lower duty cycles are all indicative of ataxia based on literature of HD rodent models (Casaca-Carreira et al., 2015; Timotius et al., 2019).

In *Kcnmal* mutant mice cohorts, *Kcnmal*^{D434G/WT} mice show no significant difference in stand index, swing duration, step cycles, duty cycles and single stance (Figure 4.3). On the other hand, *Kcnmal*^{N999S/WT} mice show a faster stand index off both forelimbs and hindlimbs than WT controls, where *Kcnmal*^{-/-} mice did not (Figure 4.3A). *Kcnmal*^{N999S/WT} mice also show longer swing duration (Figure 4.3C) like *Kcnmal*^{-/-} mice, but only in the forelimbs. Additionally, *Kcnmal*^{N999S/WT} mice show a longer step cycle (Figure 4.3D) and single stance duration (Figure 4.3F), once again only in the forelimbs.

The longer swing speed solely accounts for the longer step cycle, as *Kcnma1*^{N999S/WT} mice do not show any significant difference in the duty cycle. Together, these parameters indicate gait disturbances in *Kcnma1*^{N999S/WT} mice, though characterization of this dysfunction is unclear. Though the combination of forelimb and hindlimb abnormalities can occur in HD rat models, there is a lack of evidence in literature indicating a classification of motor dysfunction in solely rodent forelimbs (Casaca-Carreira et al., 2015). This forelimb gait disturbance is also difficult to relate to *KCNMA1* PNKD patient symptoms as humans are not weight-bearing on the forelimbs.

Figure 4.3. *Kcnma1*^{N999S/WT} and *Kcnma1*^{-/-} mice show gait disturbances in forelimb and hindlimb parameters respectively. CatWalk gait analysis parameters. Unpaired t-test with Welch's correction performed on all groups. *Left: Kcnma1*^{N999S/WT} cohort (n=10, *Kcnma1*^{WT/WT}; n=11, *Kcnma1*^{N999S/WT}). (A) *Kcnma1*^{N999S/WT} mice show higher stand index of forelimbs (p=0.0247) and hindlimbs (p=0.0212); (B) longer swing duration of forelimbs (p=0.0008) but no significant difference in in hindlimbs (p=0.4484); (C) longer step cycle duration of forelimbs (p=0.0238) but no significant difference in in hindlimbs (p=0.1288); (D) no significant difference in duty cycles of forelimbs (p=0.4485) and hindlimbs (p=0.4539); (E) longer single stance duration of forelimbs (p=0.0012) but no significant difference in in hindlimbs (p=0.6674). *Middle: Kcnma1*^{D434G/WT} cohort (n=11, *Kcnma1*^{WT/WT}; n=9, *Kcnma1*^{D434G/WT}). (A) *Kcnma1*^{D434G/WT} mice show no significant difference in stand index of forelimbs (p=0.5447) and hindlimbs (p=0.3855); (B) no significant difference in swing duration of forelimbs (p=0.1593) and hindlimbs (p=0.8164); (C) no significant difference in step cycle duration of forelimbs (p=0.2143) and hindlimbs (p=0.6956); (D) no significant difference in duty cycles of forelimbs (p=0.9969) and hindlimbs (p=0.6050); (E) no significant difference in single stance duration of forelimbs (p=0.1153) and hindlimbs (p=0.3463). *Right: Kcnma1*^{-/-} cohort (n=6, *Kcnma1*^{+/+}; n=12, *Kcnma1*^{-/-}; n=6, *Kcnma1*^{-/-}). (A) *Kcnma1*^{-/-} mice show no significant difference in stand index of forelimbs (p=0.4691) and hindlimbs (p=0.6508); (B) no significant difference in swing speed duration of forelimbs (p=0.4510) but longer in hindlimbs (p=0.0462); (C) no significant difference in step cycle duration of forelimbs (p=0.4607) and hindlimbs (p=0.8150); (D) no significant difference in duty cycles of forelimbs (p=0.8771) but lower in hindlimbs (p=0.0185); (E) no significant difference in single stance duration of forelimbs (p=0.8259) and hindlimbs (p=0.2471).



From free-running wheel activity analysis, *Kcnma1* mutant mice experiencing ‘drop attack’-like paroxysms would be expected to show lower average speed. This would be correlated with more frequent gaps in wheel activity due to immobile nature of ‘drop attack’ paroxysms. On the other hand, *Kcnma1*^{-/-} mice would be expected to show lower average speed as well. This would be due to the baseline ataxic phenotype of *Kcnma1*^{-/-} mice causing locomotor dysfunction, as with HD mice wheel activity (Hickey et al., 2008; Mandillo et al., 2014). Though not directly observed (i.e., via video recording), this could

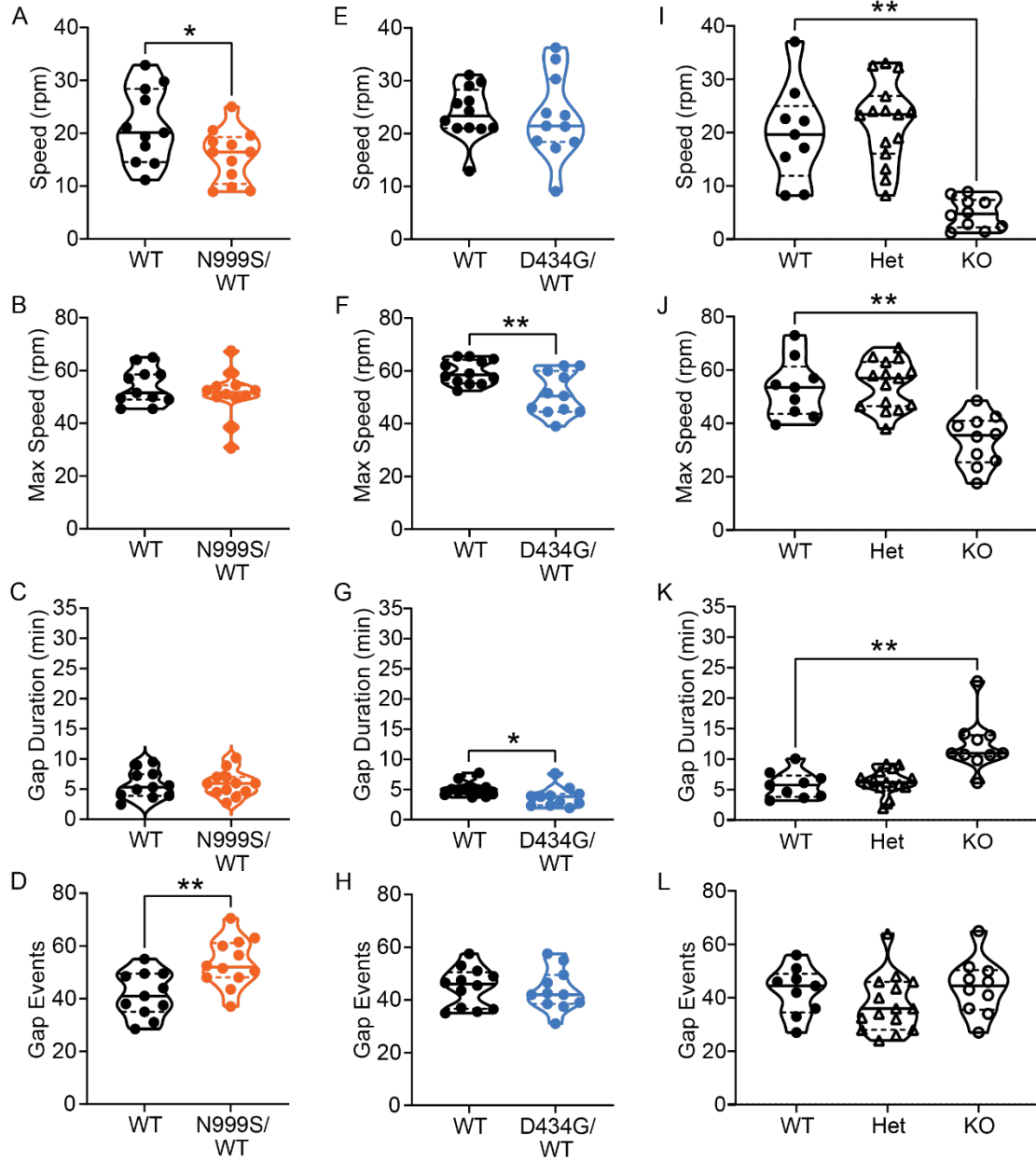
suggest a distinction between baseline and paroxysmal dyskinesia between *Kcnma1* mutant and *Kcnma1*^{-/-} groups.

From the data, *Kcnma1*^{N999S/WT} mice show a decrease in average speed (Figure 4.4A) and activity gap frequency (Figure 4.4D). No significant difference to WT controls is seen in either maximum speed (Figure 4.4B) or the activity gap duration (Figure 4.4C). Because of this, the lower average speed of *Kcnma1*^{WT/N999S} mice can likely be accounted solely by the higher activity gap frequency. For *Kcnma1*^{D434G/WT} mice, both average speed (Figure 4.4E) and the activity gap frequency (Figure 4.4H) are not significantly different to WT controls. However, there is a decrease in the maximum speed of *Kcnma1*^{D434G/WT} mice (Figure 4.4F) and activity gap duration (Figure 4.4G). As there is no significant difference in average speed or activity gap frequency, it is unclear what the decrease in maximum speed could indicate, especially since *Kcnma1*^{D434G/WT} mice had a lower activity gap duration indicating longer wheel activity.

Kcnma1^{-/-} mice show motor deficits in three of the four primary parameters analyzed from wheel activity data. Like *Kcnma1*^{N999S/WT} mice, *Kcnma1*^{-/-} mice show lower average speed (Figure 4.4I). Additionally, *Kcnma1*^{-/-} mice show lower maximum speed (Figure 4.4J) similar to *Kcnma1*^{D434G/WT} mice, but higher activity gap duration (Figure 4.4K). This indicates that *Kcnma1*^{-/-} mice are not active on wheels as frequently as *Kcnma1*^{-/+} and *Kcnma1*^{+/+} mice. When they are on wheels, they show less activity overall. This results in a 9.26 rpm greater mean difference in average speed of *Kcnma1*^{-/-} mice and their WT controls compared to the *Kcnma1*^{N999S/WT} cohort. However, *Kcnma1*^{-/-}, *Kcnma1*^{-/+} and *Kcnma1*^{+/+} mice show no significant difference in the activity gap frequency (Figure 4.4L). *Kcnma1*^{-/+} mice show no significant difference to *Kcnma1*^{+/+} mice in all parameters.

Overall, these activity deficits indicate that *Kcnmal*^{-/-} mice have a more severe motor deficit in wheel activity than *Kcnmal*^{N999S/WT} mice. Though it follows that *Kcnmal*^{N999S/WT} mice could have more frequent activity gaps from ‘drop attack’-like paroxysms, it is unclear whether these data indicate a baseline or paroxysmal phenotype without video-recording assessment.

Figure 4.4. *Kcnmal*^{N999S/WT} and *Kcnmal*^{-/-} mice show wheel activity deficits. Free-running wheel activity parameters. One-way ANOVA with Welch’s correction performed for *Kcnmal*^{-/-} group analysis. Dunnett’s T3 post-hoc test performed for multiple comparison. Unpaired t-test with Welch’s correction performed for *Kcnmal*^{D434G/WT} and *Kcnmal*^{N999S/WT} group analysis. (A-D) *Kcnmal*^{N999S/WT} cohort (n=11, *Kcnmal*^{WT/WT}; n=12, *Kcnmal*^{N999S/WT}). (A) *Kcnmal*^{N999S/WT} mice show lower average speed (p=0.0411). (B) *Kcnmal*^{N999S/WT} mice show no significant difference in average maximum speed to WT controls (p=0.3618). (C) *Kcnmal*^{N999S/WT} mice show no significant difference in average activity gap duration to WT controls (p=0.8281). (D) *Kcnmal*^{N999S/WT} mice show lower frequency of activity gap events (p=0.0040). (E-H) *Kcnmal*^{D434G/WT} cohort (n=12, *Kcnmal*^{WT/WT}; n=11, *Kcnmal*^{D434G/WT}). (E) *Kcnmal*^{D434G/WT} mice show no significant difference in average speed to WT controls (p=0.8118). (F) *Kcnmal*^{D434G/WT} mice show lower average maximum speed (p=0.0085). (G) *Kcnmal*^{D434G/WT} mice show lower average activity gap duration (p=0.0467). (H) *Kcnmal*^{D434G/WT} mice show no significant difference in frequency of activity gap events to WT controls (p=0.7425). (I-L) *Kcnmal*^{-/-} cohort (n=9, *Kcnmal*^{+/+}; n=15, *Kcnmal*^{-/+}; n=10, *Kcnmal*^{-/-}). (I) *Kcnmal*^{-/-} mice show lower average speed than *Kcnmal*^{+/+} mice (p=0.0032), while *Kcnmal*^{-/+} mice show no significant difference to *Kcnmal*^{+/+} mice (p=0.9057) (p<0.0001 main effect). (J) *Kcnmal*^{-/-} mice show lower average maximum speed than *Kcnmal*^{+/+} mice (p=0.0024), while *Kcnmal*^{-/+} mice show no significant difference to *Kcnmal*^{+/+} mice (p=0.9871) (p=0.0001 main effect). (K) *Kcnmal*^{-/-} mice showed higher average activity gap duration than *Kcnmal*^{+/+} mice (p=0.0026), while *Kcnmal*^{-/+} mice show no significant difference to *Kcnmal*^{+/+} mice (p=0.8987) (p=0.0023 main effect). (L) *Kcnmal*^{-/-} mice show no significant difference in frequency of activity gap events to *Kcnmal*^{+/+} mice (p=0.9800), while *Kcnmal*^{-/+} mice also show no significant difference to *Kcnmal*^{+/+} mice (p=0.5565) (p=0.3047 main effect).



In the restraint-induced dyskinesia assay, *Kcnma1* mutant mice would be expected to show longer immobility due to an acute stressor triggering ‘drop attack’-like paroxysms. This could in turn result in lower stereotypic behavior, though large abnormal dyskinetic movement is not expected. With baseline dyskinesia phenotypes, *Kcnma1*^{-/-} mice would be expected to show continuous tremors and hyperactivity through the 5-minute recording,

resulting in shorter immobility. Like *KCNMA1* patient ‘drop attacks’, stress-induced periods of immobility could suggest a paroxysmal dyskinesia as opposed to the baseline dyskinesia of *Kcnmal*^{+/-} mice.

From post-restraint video analysis, WT mice from all groups show normal exploratory behavior including sniffing, grooming and rearing with coordinated movements. All *Kcnmal* mutant and *Kcnmal*^{+/-} mice did not show any choreiform movements or collapsing behavior (all four paws no longer touching the ground). *Kcnmal*^{N999S/WT} mice show longer immobility (Figure 4.5A) with no significant difference in numbers of total rears (Figure 4.5B) and bins of grooming (Figure 4.5C) to WT controls. Immobility in all *Kcnmal*^{N999S/WT} mice was not continuous, but rather occurred in periods of immobility that were discontinued with exploratory behavior similar to WT controls. Three male *Kcnmal*^{N999S/WT} mice show tonic-clonic movements resembling a myoclonic “hiccup” throughout immobility periods that were not associated with respiratory rates (Appendix Video 1). On the other hand, WT mice hold a less hunched posture with their heads raised higher during immobility, suggesting a more bright and alert status (Appendix Figure 2). This posturing and myoclonic movement is also seen in only one WT control and occurs at shorter durations than *Kcnmal*^{N999S/WT} mice. One male *Kcnmal*^{N999S/WT} shows sideways listing during the first bin of scoring. And finally, one male *Kcnmal*^{N999S/WT} mouse, two female *Kcnmal*^{N999S/WT} mice and one WT control hold flattened postures during the first bin of scoring. *Kcnmal*^{D434G/WT} mice did not show significant differences in immobility (Figure 4.5D), total number of rears (Figure 4.5B) or bins of grooming (Figure 4.5C) compared to WT controls. One female *Kcnmal*^{D434G/WT}

mouse shows listing in the first bin of scoring and another female *Kcnma1*^{D434G/WT} mouse holds a flattened posture through the first two bins of scoring.

For this assay, the *Kcnma1*^{-/-} group is underpowered, as sample sizes of at least n=5 for *Kcnma1*^{-/-} and *Kcnma1*^{+/+} mice are needed to achieve sufficient power for appropriate statistical analysis of dyskinesia scoring. However, three out of four *Kcnma1*^{-/-} mice show shorter immobility (Figure 4.5G) and all four *Kcnma1*^{-/-} mice show lower scored 30 second bins of grooming (Figure 4.5C). Three out of four *Kcnma1*^{-/-} mice show hyperactivity through circling and rapid limb movements, and one *Kcnma1*^{-/-} mouse shows a visible tremor during brief immobility periods. Though not statistically significant, this is likely indicative of abnormal dyskinetic movements at baseline, such as known tremor and ataxia, causing a presentation of hyperactivity in *Kcnma1*^{-/-} mice. These findings are corroborated by ongoing testing to increase the *Kcnma1*^{-/-} cohort sample size (data not shown). This indicates a distinct behavioral phenotype difference between *Kcnma1*^{N999S/WT} and *Kcnma1*^{-/-} mice. Where *Kcnma1*^{-/-} mice show continuous movement from baseline tremors and hyperactivity, *Kcnma1*^{N999S/WT} show longer periods of immobility suggesting a possible ‘drop attack’-like paroxysmal dyskinesia.

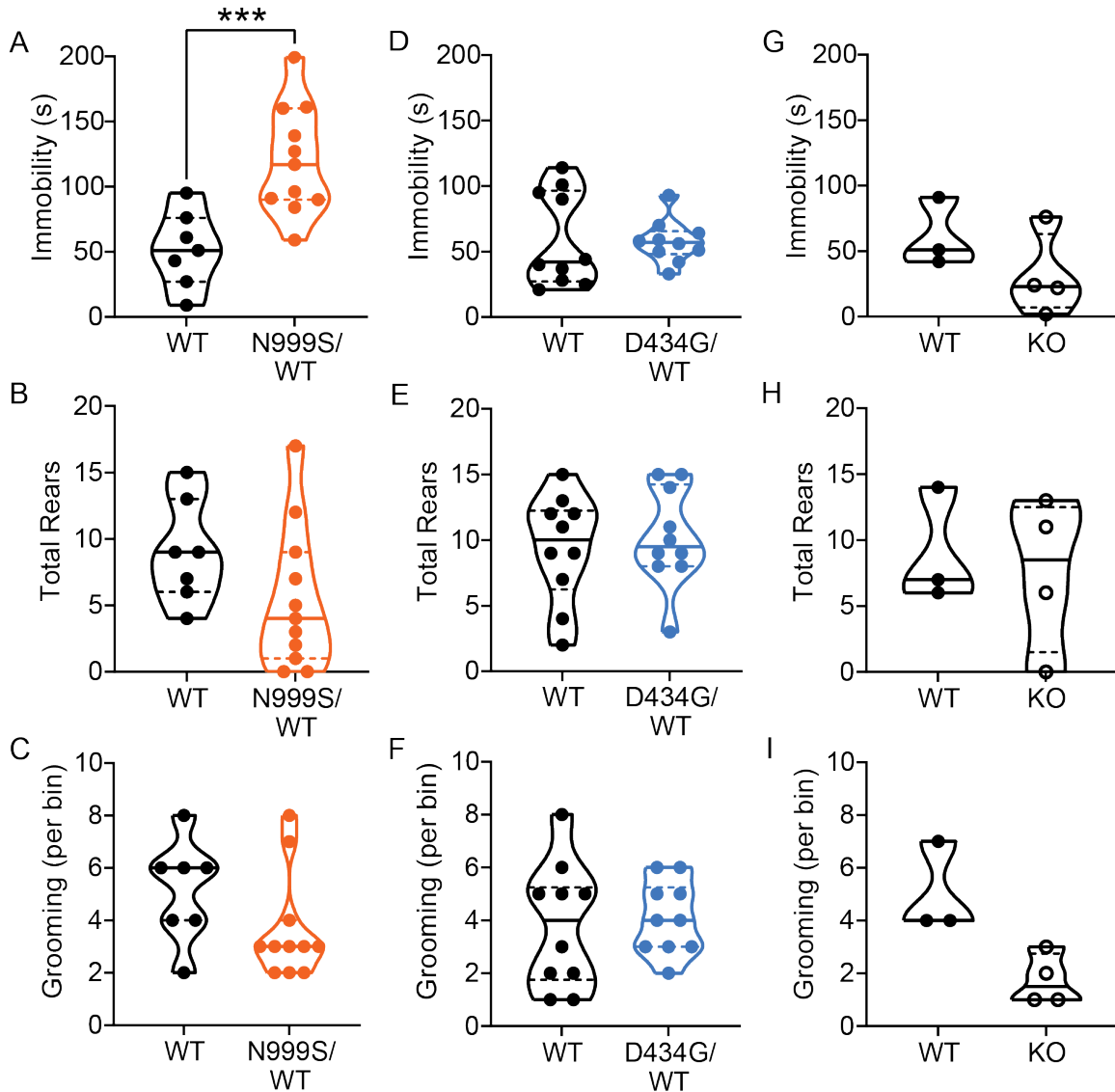


Figure 4.5. *Kcnma1*^{N999S/WT} mice longer immobility time. Restraint-induced dyskinesia analysis and scoring. Unpaired Welch's t-test performed on all groups. (A-C) *Kcnma1*^{N999S/WT} cohort (n=7, *Kcnma1*^{WT/WT}; n=11, *Kcnma1*^{N999S/WT}). (A) *Kcnma1*^{N999S/WT} mice show longer immobility (p=0.0008). (B) *Kcnma1*^{N999S/WT} mice show no significant difference in total number of rears to WT controls (p=0.1251). (C) *Kcnma1*^{N999S/WT} mice show no significant difference in grooming per bin to WT controls (p=0.1384). (D-F) *Kcnma1*^{D434G/WT} cohort (n=10, *Kcnma1*^{WT/WT}; n=10, *Kcnma1*^{D434G/WT}). (D) *Kcnma1*^{D434G/WT} mice show no significant difference in immobility to WT controls (p=0.8817). (E) *Kcnma1*^{D434G/WT} mice no significant difference in total number of rears to WT controls (p=0.6533). (F) *Kcnma1*^{D434G/WT} mice no significant difference in grooming per bin to WT controls (p=0.7321). (G-I) *Kcnma1*^{-/-} cohort (n=3, *Kcnma1*^{+/+}; n=4, *Kcnma1*^{-/-}). (G) *Kcnma1*^{-/-} mice show no significant difference in immobility to WT controls (p=0.2247). (H) *Kcnma1*^{-/-} mice show no significant difference in total number of rears to WT controls (p=0.7123). (I) *Kcnma1*^{-/-} mice show no significant difference in total grooming per bin to WT controls (p=0.0630).

CHAPTER 5: DISCUSSION

5.1. General Discussion

Following the hypothesis that *KCNMA1* variants cause dyskinesia in mice, there is little evidence to indicate that *Kcnma1*^{D434G/WT} mice show a dyskinesia phenotype. Where *Kcnma1*^{D434G/WT} mice do show significant differences to WT controls, indication of motor dysfunction is unclear. For instance, from free-running wheel activity, *Kcnma1*^{D434G/WT} mice show lower maximum speed but lower activity gap durations as well. These two parameters, while significantly different to WT controls, conflict in their indications of dyskinesia. This is unlike *Kcnma1*^{N999S/WT} mice, which show motor deficits across all assays with immobility during the restraint-induced dyskinesia assay. Similarly, *Kcnma1*^{-/-} mice show motor deficits across all assays with higher severity compared to *Kcnma1*^{N999S/WT} mice. *Kcnma1*^{-/-} mice show lower fall latency times and impaired motor learning in elicited assays, as well as lower wheel activity. *Kcnma1*^{-/-} mice also trend towards showing shorter immobility than WT controls, likely due to their baseline tremors and hyperactivity. **This suggests that both *Kcnma1*^{N999S/WT} and *Kcnma1*^{-/-} mice show motor dysfunction that is likely associated with abnormal involuntary movements or immobility indicative of dyskinesia.**

Unlike hanging wire, rotarod, CatWalk and wheel activity assays, the restraint-induced dyskinesia assay provides a unique phenotype of immobility in *Kcnma1*^{N999S/WT} mice. Out of all motor assays performed, this lack of movement observed from restraint-induced stress most closely resembles the PNKD ‘drop attack’ phenotype of N999S patients. Additionally, the restraint-induced dyskinesia assay has the potential to delineate between a baseline and paroxysmal dyskinesia. *Kcnma1*^{-/-} mice show baseline dyskinesia

in ataxia and tremors which may correlate observed hyperactivity and shorter immobility. On the other hand, *Kcnma1*^{N999S/WT} mice show longer periods of immobility that are broken up by periods of normal exploratory behavior. These discontinuous periods of immobility more resemble paroxysms of dyskinesia than baseline phenotypes. Thus, qualitative and quantitative assessment of immobility through this assay have the potential to distinguish between a baseline and paroxysmal dyskinesia.

Among the other motor assays, *Kcnma1*^{N999S/WT} mice show deficits in hanging wire, rotarod, CatWalk and wheel activity analysis. The CatWalk analysis shows gait disturbances in only the forelimbs, making it difficult to characterize a specific motor dysfunction, like *Kcnma1*^{-/-} ataxia. It is also difficult to further characterize these *Kcnma1*^{N999S/WT} mice phenotypes as resembling *KCNMA1* patient ‘drop attacks’ as these assays cannot delineate between a baseline and paroxysmal dyskinesia. Though *Kcnma1*^{-/-} mice show a more severe baseline phenotype, *Kcnma1*^{N999S/WT} mice show similar results across rotarod, hanging wire and wheel activity assays. Thus, unlike the restraint-induced dyskinesia assay, association with baseline phenotypes cannot be ruled out from these assays.

It is worth noting that no case reports of N999S or D434G patients thus far have described any baseline dyskinesia phenotype (Bailey et al., 2019; Heim et al., 2020; Keros et al., 2021; Miller et al., 2021; Wang et al., 2017). As elicited motor assays, CatWalk and wheel activity indicate possible *Kcnma1*^{N999S/WT} baseline motor deficits, these results could suggest a unique baseline phenotype that has yet to be characterized in *KCNMA1* PNKD patients. However, relating these baseline motor assay results to *currently* observed *KCNMA1* patient phenotypes makes it unclear whether the N999S mutation cause

KCNMA1 PNKD ‘drop attacks’ in mice.

Few mouse models of PNKD, let alone *KCNMA1*-specific PNKD, exist showing an established genotype-phenotype relation to compare to *Kcnmal*^{N999S/WT} mice. Because of this, interpretations of results are limited by the resource restrictions of this thesis study without comparisons to prior models. Additionally, mouse models of paroxysmal dyskinesia, such as Ca²⁺ channelopathies, *PRRT2*-deficient/KO and *PNKD* mutant mice, are not characterized well in relation to patient phenotypes through similar motor assays. Even with these models showing more distinct dyskinesias defined by chorea and dystonia, prior motor assays provide little characterization of paroxysms beyond dyskinesia scoring (Fureman et al., 2002; Khan et al., 2004; Khan and Jinnah, 2002; Lee et al., 2012; Michetti et al., 2017; Shirley et al., 2008; Tan et al., 2018). This makes relating patient phenotypes to these mouse models difficult, especially when paroxysm triggers and EEG-determined epileptic status are unknown. Ca²⁺ channelopathy *Tottering* mice show paroxysms that are provoked by caffeine and ethanol injection as well as stress-induction, similar to triggers of some PNKD types (Fureman et al., 2002; McGuire et al., 2018). However, these mice, along with *PRRT2*-deficient/KO and *PNKD* mutant models, do not show paroxysms resembling the *KCNMA1* PNKD ‘drop attacks’ seen in N999S patients. Ca²⁺ channelopathy, *PRRT2*-deficient/KO and *PNKD* mutant mice generally show dyskinetic movement as opposed to a lack of movement seen in *KCNMA1* patient ‘drop attacks.’ (Fureman et al., 2002; Heim et al., 2020; J. Heim, 2019; Lee et al., 2012; Michetti et al., 2017; Miller et al., 2021; Tan et al., 2018).

Recently, a study of *drosophila* harboring an orthologous mutation to the *KCNMA1* D434G variant shows changes in locomotor behavior. Also, *Kcnmal* mutant *drosophila*

show leg twitches in clustered bouts. These changes are associated with changes in AP waveform and reduced Ca^{2+} neurotransmitter release (Kratschmer et al., 2021). However, relating these results to the human *KCNMA1* patient phenotypes can be difficult. First, the orthologous mutation shows a higher BK channel sensitivity to Ca^{2+} and voltage than heterologous expression of the D434G mutation in cells. This sensitivity difference could present as a different phenotype in *drosophila*. Second, locomotor changes were quantified through tracking of movement using parameters such as distance travelled and infrared beam breaks. Like the wheel activity assay, differences in locomotion can be indicative of dyskinesia, but cannot distinguish between baseline and paroxysmal dyskinesia. Finally, leg twitches are not the primary phenotype of PNKD observed in human *KCNMA1* patients (Bailey et al., 2019; Heim et al., 2020; Miller et al., 2021). For these reasons, this *drosophila* model does not fully represent a genotype-phenotype relation of *KCNMA1* mutations. The D434G mutant mouse of Dong et al., 2021 could potentially be a more accurate model of human *KCNMA1* patient phenotypes. However, D434G mutant mice were only tested on assays that also cannot distinguish between baseline and paroxysmal dyskinesia, such as rotarod and gait analysis. This mouse model provides a comparison of baseline motor dysfunction in *Kcnmal* mutant mice, but lacks evidence of human phenotype recapitulation.

5.2. Future Direction

It is yet to be determined whether this immobility in *Kcnmal*^{N999S/WT} mice is associated with absence/tonic seizures, a fear response or a novel paroxysmal trigger. Simultaneous EEG analysis of mice during the restraint-induced dyskinesia assay is

necessary to determine absence/tonic seizure association. Dyskinesia is defined by abnormal, involuntary movements with a *lack* of seizure activity. Without EEG monitoring, seizure activity and dyskinesia cannot be distinguished.

Next, freezing response from fear could present as periods of immobility. A previous study shows fear-conditioned freezing responses in mice are associated with increases in neuronal excitability of lateral amygdala neurons through BK channel activity suppression (Sun et al., 2015). However, the N999S variant is a GOF mutation which could mechanistically act different in amygdaloid circuits compared to LOF channel activity suppression (Li et al., 2018; Moldenhauer et al., 2020). Additionally, this study used a fear-conditioning paradigm without observing non-conditioned freezing response from acute changes in BK channel activity, such as pharmacologic channel blockers (Sun et al., 2015). The restraint-induced dyskinesia assay investigates acute stress response and does not qualify as a fear-conditioning paradigm as mice are under a novel restraint for only 5 minutes. And because fear-conditioned paradigms are more prevalent in measuring freezing responses, there is a lack of literature on freezing responses from acute novel stress. This imposes a difficulty in evaluating normal freezing responses under such conditions. Additionally, the open field assay can detect anxiety-like behavior by measuring the total distance travelled by mice from spontaneous movement in a large, enclosed area (Crawley, 2000). Preliminary findings show that *Kcnma1*^{N999S/WT} mice show no significant difference in distance travelled compared to WT controls (data not shown). This suggests that *Kcnma1*^{N999S/WT} mice do not show spontaneous freezing behaviors.

Finally, *Kcnma1*^{N999S/WT} do not exhibit any qualitative immobility upon everyday caretaking observation. However, analysis of *Kcnma1*^{N999S/WT} and *Kcnma1*^{-/-} mice video-

recorded in the beaker without an acute stressor is needed to test whether stress is triggering longer immobility in *Kcnma1*^{N999S/WT} mice. Without a non-stressed control group, it is unclear whether this *Kcnma1*^{N999S/WT} immobility is a paroxysmal dyskinesia triggered by stress or a dyskinesia with no, or unknown, paroxysmal trigger. While the higher immobility of *Kcnma1*^{N999S/WT} mice shares semblance to *KCNMA1* PNKD ‘drop attacks’, it is difficult to distinguish it from other possible behaviors without further investigation.

Although not fully characterized, the immobility seen in *Kcnma1*^{N999S/WT} mice may provide the possibility for treatment investigation. Anti-seizure medications are recommended for treatment of *KCNMA1*-linked channelopathy associated PNKD, though only some *KCNMA1* patients show associations with epilepsy. This is largely due to a lack of FDA approved BK channel pharmacological modulators and/or a misdiagnosis of PNKD as being epilepsy (Bailey et al., 2019). On anti-seizure medication, one N999S patient showed PNKD paroxysms further provoked by oxcarbazepine, typically used for absence seizure treatment (Wang et al., 2017). The wide range of efficacy in anti-seizure medications reported from other patient cases and possible severe negative side effects indicate a need for research in better treatment options (Bailey et al., 2019; Du et al., 2005; J. Heim, 2019; Li et al., 2018; Wang et al., 2017). Recently, case studies of N999S patients show positive response to lisdexamfetamine (Vyvanse) stimulant therapy (Keros et al., 2021). Though the mechanism of action is unknown, PNKD paroxysms were significantly reduced from baseline in all patients. Patient cases associated with epilepsy did not experience any worsening seizure activity.

Due to the positive response seen in N999S patients, consideration should be given to investigating this stimulant therapy in *Kcnma1*^{N999S/WT} mice. Stimulant therapy testing

in *Kcnma1*^{N999S/WT} mice could prove beneficial through a modified restraint-induced dyskinesia assay developed from this thesis study. Injection of stimulant drug after baseline dyskinesia scoring of restraint-induced dyskinesia could result in a recovery of lengthy immobility periods in *Kcnma1*^{N999S/WT} mice. Additional EEG monitoring can also be done simultaneously to assess if immobility is associated with seizure activity. This could not only recapitulate the stimulant results of N999S patient cases, but could also give further support that long periods of immobility in *Kcnma1*^{N999S/WT} mice are indeed PNKD paroxysms. In turn, this stimulant assay could pave the path in investigating electrophysiologic and pharmacologic mechanisms for further characterization and treatment of *KCNMA1*-linked channelopathy.

APPENDIX 1: BK CHANNELS EXPRESSION

Appendix Table 1. BK channel motor phenotype associations in cellular and animal models across the central and peripheral nervous system.

Nervous System	Location	Cell/Neuron Type	BK Channel Motor Phenotype Associations	Source
Central	Cerebellum	Purkinje	Motor control, coordination, BK channel KO associated with ataxia in <i>Kcna1</i> ^{-/-} mice	(Chen et al., 2010; Meredith et al., 2004; Sausbier et al., 2004)
	Superchiasmatic nucleus (hypothalamus)	Superchiasmatic (SCN)	Pacemaker output and diurnal excitability of circadian rhythm	(Kent and Meredith, 2008; Meredith et al., 2006; Montgomery et al., 2013; White et al., 2014; Whitt et al., 2016)
	Cingulate cortex & amygdala	Cortical pyramidal & lateral amygdala (LAN)	Fear-conditioning and depression-like behavior	(Sun et al., 2011; Sun et al., 2015)
	Hippocampus	Hippocampal pyramidal & dentate granules (DGN)	Learning, memory and epileptic disorders	(Choi et al., 2018; Ermolinsky et al., 2008; Mehranfard et al., 2014, 2015; Typlt et al., 2013)

Appendix Table 1 Continued

	Striatum	Cholinergic interneurons	BK channels contribute to regulation of spontaneous firing and fAHP's	(Goldberg and Wilson, 2005; Rueda-Orozco and Robbe, 2015; Wilson and Goldberg, 2006)
	Somatosensory Cortex	Cortical pyramidal	Seizure-induced GOF in BK channels and <i>NIPA2</i> KO mice associated with increases in neuronal excitability	(Benhassine and Berger, 2009; Gómez et al., 2021; Liu et al., 2019; Shruti et al., 2008)
Peripheral	Neuromuscular junction (NMJ)	Motor neuron/muscle fiber junction	Regulation of synaptic depression, AP repolarization and Ca ²⁺ -dependent pre-synaptic vesicle release. Associated with <i>Kcnmal</i> ^{-/-} mice muscle weakness	(Ford and Davis, 2014; Pattillo et al., 2001; Robitaille and Charlton, 1992; Vatanpour and Harvey, 1995; Wang et al., 2020)
	Skeletal muscle	Myoblasts, slow/fast twitch muscle fibers	Regulation of myoblast proliferation/migration associated with myotonic dystrophy. <i>Kcnmal</i> ^{-/-} mice associated with muscle atrophy	(Dinardo et al., 2012; Maqoud et al., 2017; Tajhya et al., 2016; Tricarico et al., 2005)

APPENDIX 2: DESCRIPTIONS OF DYSKINESIA RODENT MODELS

Appendix Table 2. Phenotype descriptions in rodent models of baseline and paroxysmal dyskinesias.

Strain	Target Gene	Phenotype	Source
R6/5/2/1	<i>HTT</i> CAG repeat	Resting tremor, movements resembling chorea, stereotypic involuntary movements and a mild ataxia. Dyskinesia/dystonia when held by tail. Severe handling-induced epileptic seizures.	(Mangiarini et al., 1996)
RGS9 KO + L-Dopa Treatment	<i>RGS9</i> KO	Abnormal motor behavior that resembles levodopa-induced dystonia and dyskinesia including excessive sideward and backward motions, difficulty maintaining an upright posture, frequent rapid jerky (tonic) movements of hindlimbs and an excessively bent trunk resembling dystonia.	(Kovoor et al., 2005; Strecker et al., 2012)
PRRT2 Deficient/ KO	<i>PRRT2</i> Stop codon at exon 2 C649	Some spontaneous dyskinesia and dystonia. Repeated administration of an initially sub-convulsive electric stimulus results in seizures followed by choreiform movements and then dystonic posturing of the trunk, limbs and tail	(Michetti et al., 2017; Tan et al., 2018)
Tottering	<i>Cacn1a</i> Ca _v 2.1 α1a subunit	Slow extension and contraction of hindlimbs. Severe flexion of upper limbs, head and neck and paddling movements of both hindlimbs. Induced by stress, caffeine, ethanol but not exertion. Associated with absence seizures.	(Fureman et al., 2002)
Rocker	<i>Cacn1a</i> Ca _v 2.1 α1a subunit	Baseline same as tottering. Attack almost all in females, reduced frequency, shorter and less severe than tottering. Dystonic flexion of one limb and limited spread before termination.	(Shirley et al., 2008)

Appendix Table 2 Continued

Lethargic	<i>Cacnb4</i> Ca _v 2.1 β4 subunit	Ataxia at baseline, circling, listing to one side, exaggerated flexion or extension of the trunk, falling, clonic limb movement with tonic extension/retraction.	(Khan and Jinnah, 2002)
Stargazer	<i>Cacng2</i> L-type Ca ²⁺ channel γ1 subunit	Circling, hyperactivity, and frequent chaotic movements of the head in both vertical and horizontal directions – absence seizures.	(Khan et al., 2004)
<i>PNKD</i> mut-TG	<i>MR-1/PNKD</i> gene A6V & A8V mutations	No baseline phenotype. Dyskinesia induced from stress, caffeine and ethanol. Oral-facial movements (e.g., tongue protrusions), stereotypic movements, severe axial stiffness (dystonia) from caffeine.	(Lee et al., 2012)

APPENDIX 3: ALL CATWALK PARAMETERS AND WEIGHT COMPARISON

Appendix Table 3. Comparison of all significant CatWalk parameters p-values across *Kcnma1*^{N999S/WT}, *Kcnma1*^{D434G/WT} and *Kcnma1*^{-/-} cohorts. All parameters represented are of statistical significance (p<0.05) in at least one of the three experimental cohorts. All paw statistics (front right, front left, hind right, hind left, forelimbs, hindlimbs) are represented when possible. For further parameter descriptions, refer to CatWalk XT manual.

	<i>Kcnma1</i> ^{N999S/WT}	<i>Kcnma1</i> ^{D434G/WT}	<i>Kcnma1</i> ^{-/-}
Stand Index (cm²/s)			
<i>Right Front</i>	0.0044	0.7947	0.3656
<i>Left Front</i>	0.1557	0.1598	0.7548
<i>Right Hind</i>	0.0187	0.6895	0.5977
<i>Left Hind</i>	0.0596	0.8949	0.1364
<i>Forelimbs</i>	0.0247	0.4123	0.5060
<i>Hindlimbs</i>	0.0212	0.7688	0.2048
Max Contact At (%)			
<i>Right Front</i>	0.4124	0.3185	0.0001
<i>Left Front</i>	0.1398	0.4607	0.0003
<i>Right Hind</i>	0.6916	0.0397	0.0616
<i>Left Hind</i>	0.9695	0.1885	0.3162
<i>Forelimbs</i>	0.2098	0.3521	0.0001
<i>Hindlimbs</i>	0.7843	0.8374	0.1183
Max Contact Area (cm²)			
<i>Right Front</i>	0.0402	0.7414	0.0243
<i>Left Front</i>	0.1120	0.3672	0.0394
<i>Right Hind</i>	0.7166	0.5841	0.0352
<i>Left Hind</i>	0.2603	0.8642	0.0233
<i>Forelimbs</i>	0.0412	0.7425	0.0253
<i>Hindlimbs</i>	0.3797	0.8615	0.0160
Max Contact Max Intensity			
<i>Right Front</i>	0.2049	0.4300	0.0991
<i>Left Front</i>	0.1058	0.1120	0.0714
<i>Right Hind</i>	0.3600	0.6639	0.0182
<i>Left Hind</i>	0.4817	0.7004	0.0427
<i>Forelimbs</i>	0.1361	0.2122	0.0751
<i>Hindlimbs</i>	0.3897	0.9812	0.0239

Appendix Table 3 Continued

Max Contact Mean Intensity			
<i>Right Front</i>	0.8653	0.5379	0.0004
<i>Left Front</i>	0.7187	0.5284	0.0001
<i>Right Hind</i>	0.9959	0.6118	0.0003
<i>Left Hind</i>	0.9857	0.2940	0.0029
<i>Forelimbs</i>	0.9300	0.5303	0.0002
<i>Hindlimbs</i>	0.8490	0.4254	0.0007
Print Length (cm)			
<i>Right Front</i>	0.4490	0.3177	0.0003
<i>Left Front</i>	0.9779	0.7151	0.0560
<i>Right Hind</i>	0.5974	0.5659	0.0489
<i>Left Hind</i>	0.4935	0.4830	0.0089
<i>Forelimbs</i>	0.6416	0.6870	0.0046
<i>Hindlimbs</i>	0.4606	0.8913	0.0038
Print Width (cm)			
<i>Right Front</i>	0.9329	0.8926	0.0126
<i>Left Front</i>	0.8528	0.0099	0.0005
<i>Right Hind</i>	0.2722	0.6995	0.0681
<i>Left Hind</i>	0.4635	0.8388	0.0085
<i>Forelimbs</i>	0.9637	0.1223	0.0005
<i>Hindlimbs</i>	0.9490	0.9282	0.0090
Print Area (cm²)			
<i>Right Front</i>	0.2975	0.6144	0.0192
<i>Left Front</i>	0.3478	0.4202	0.0488
<i>Right Hind</i>	0.7417	0.8235	0.0604
<i>Left Hind</i>	0.3837	0.9653	0.0271
<i>Forelimbs</i>	0.2802	0.8692	0.0261
<i>Hindlimbs</i>	0.4819	0.9271	0.0219
Max Intensity At (%)			
<i>Right Front</i>	0.9790	0.4971	0.0375
<i>Left Front</i>	0.1202	0.9198	0.1238
<i>Right Hind</i>	0.8460	0.7336	0.2240
<i>Left Hind</i>	0.1295	0.4078	0.0296
<i>Forelimbs</i>	0.3062	0.7337	0.0446
<i>Hindlimbs</i>	0.4035	0.5413	0.0349

Appendix Table 3 Continued

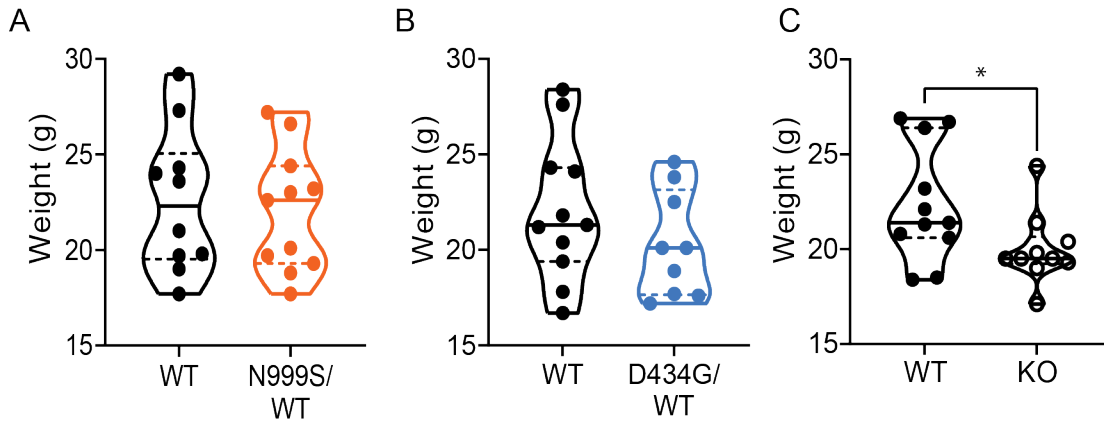
Max Intensity			
<i>Right Front</i>	0.2029	0.6238	0.0767
<i>Left Front</i>	0.1804	0.0619	0.0633
<i>Right Hind</i>	0.3758	0.6767	0.0192
<i>Left Hind</i>	0.4183	0.5291	0.0276
<i>Forelimbs</i>	0.1818	0.2370	0.0651
<i>Hindlimbs</i>	0.3731	0.9122	0.0184
Min Intensity			
<i>Right Front</i>	0.9916	0.6001	0.0001
<i>Left Front</i>	0.9866	0.6279	0.0001
<i>Right Hind</i>	0.7912	0.7337	0.0001
<i>Left Hind</i>	0.6063	0.5137	0.0001
<i>Forelimbs</i>	0.9891	0.6139	0.0001
<i>Hindlimbs</i>	0.9041	0.6090	0.0001
Mean Intensity			
<i>Right Front</i>	0.9040	0.5653	0.0003
<i>Left Front</i>	0.9014	0.5012	0.0001
<i>Right Hind</i>	0.8036	0.7354	0.0003
<i>Left Hind</i>	0.9990	0.2890	0.0013
<i>Forelimbs</i>	0.9993	0.5298	0.0001
<i>Hindlimbs</i>	0.9014	0.4861	0.0004
Mean Intensity of the 15 Most Intense Pixels			
<i>Right Front</i>	0.3778	0.6384	0.0109
<i>Left Front</i>	0.4165	0.2557	0.0073
<i>Right Hind</i>	0.6389	0.9899	0.0048
<i>Left Hind</i>	0.5016	0.4481	0.0103
<i>Forelimbs</i>	0.3867	0.4156	0.0079
<i>Hindlimbs</i>	0.5440	0.6762	0.0053
Swing (s)			
<i>Right Front</i>	0.0035	0.2256	0.5048
<i>Left Front</i>	0.0017	0.2428	0.4572
<i>Right Hind</i>	0.3858	0.7679	0.0923
<i>Left Hind</i>	0.9382	0.5702	0.0493
<i>Forelimbs</i>	0.0008	0.1593	0.4510
<i>Hindlimbs</i>	0.4484	0.8164	0.0462

Appendix Table 3 Continued

Swing Speed (cm/s)			
<i>Right Front</i>	0.0565	0.2684	0.1415
<i>Left Front</i>	0.1142	0.5152	0.2194
<i>Right Hind</i>	0.4253	0.7882	0.0680
<i>Left Hind</i>	0.3390	0.7055	0.0115
<i>Forelimbs</i>	0.0741	0.3053	0.1472
<i>Hindlimbs</i>	0.3219	0.9353	0.0121
Stride Length (cm)			
<i>Right Front</i>	0.3164	0.7996	0.9487
<i>Left Front</i>	0.3691	0.7776	0.7541
<i>Right Hind</i>	0.3616	0.9869	0.8746
<i>Left Hind</i>	0.1623	0.5941	0.4707
<i>Forelimbs</i>	0.3353	0.7832	0.9139
<i>Hindlimbs</i>	0.2174	0.7005	0.7134
Step Cycle (s)			
<i>Right Front</i>	0.0268	0.2976	0.3745
<i>Left Front</i>	0.0270	0.1632	0.5809
<i>Right Hind</i>	0.1372	0.5200	0.4396
<i>Left Hind</i>	0.2248	0.9640	0.8702
<i>Forelimbs</i>	0.0238	0.2143	0.4607
<i>Hindlimbs</i>	0.1288	0.6956	0.8150
Duty Cycle (%)			
<i>Right Front</i>	0.2705	0.7332	0.9552
<i>Left Front</i>	0.8973	0.5059	0.4572
<i>Right Hind</i>	0.4342	0.5902	0.0923
<i>Left Hind</i>	0.7731	0.7194	0.0493
<i>Forelimbs</i>	0.4485	0.9969	0.8771
<i>Hindlimbs</i>	0.5405	0.6050	0.0185
Single Stance (s)			
<i>Right Front</i>	0.0276	0.3443	0.5936
<i>Left Front</i>	0.0009	0.0885	0.8197
<i>Right Hind</i>	0.3159	0.5696	0.8636
<i>Left Hind</i>	0.5551	0.4492	0.0810
<i>Forelimbs</i>	0.0012	0.1153	0.8259
<i>Hindlimbs</i>	0.6674	0.3463	0.2471

Appendix Table 3 Continued

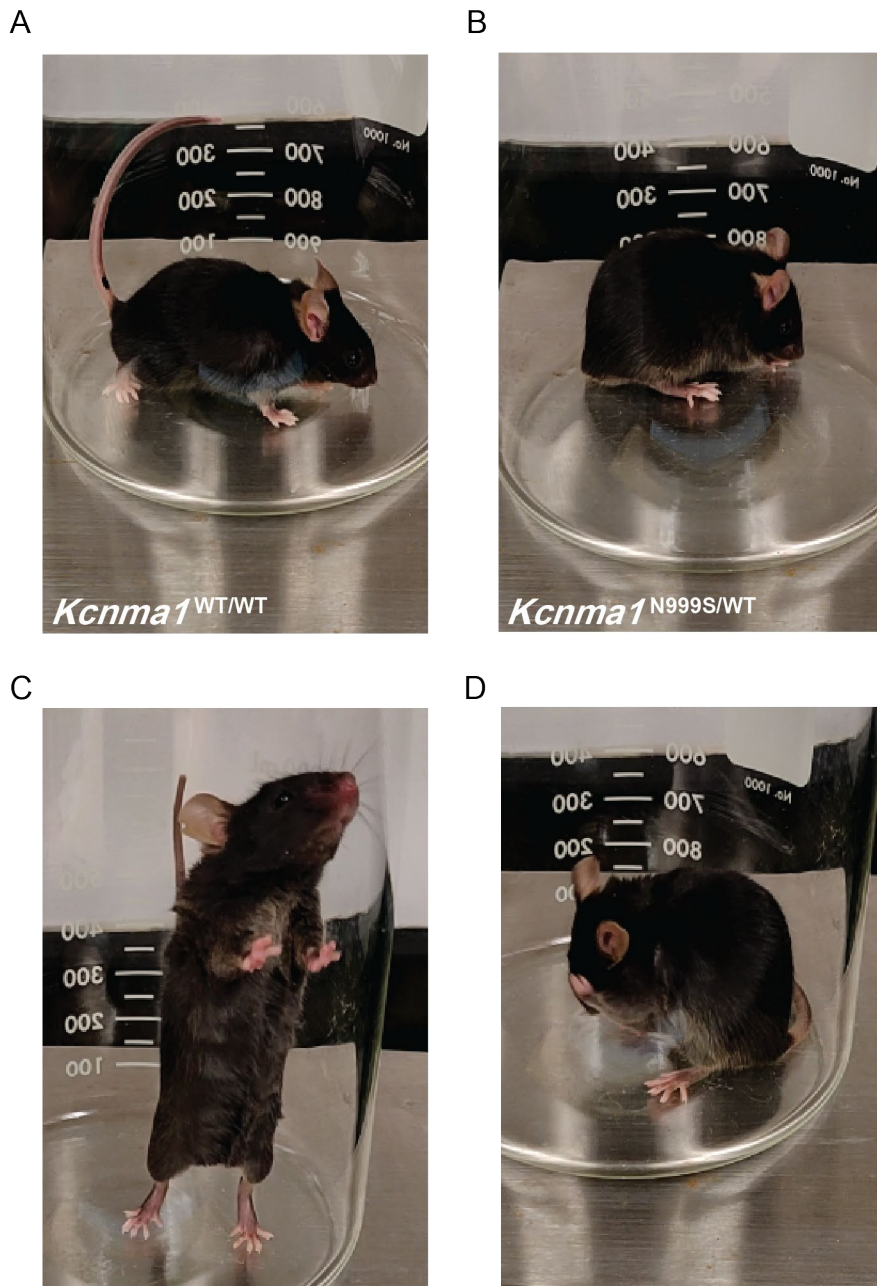
Terminal Dual Stance (s)			
<i>Right Front</i>	0.5016	0.4677	0.2916
<i>Left Front</i>	0.4280	0.5951	0.7845
<i>Right Hind</i>	0.3988	0.2862	0.8822
<i>Left Hind</i>	0.0254	0.7143	0.4607
<i>Forelimbs</i>	0.4486	0.9266	0.4737
<i>Hindlimbs</i>	0.1317	0.4631	0.6882
Base of Support (cm)			
<i>Forelimbs</i>	0.6530	0.8688	0.0029
<i>Hindlimbs</i>	0.4837	0.4728	0.0105
Other Parameters			
Regularity Index (%)	0.0141	0.2804	0.1681
Cadence	0.0259	0.5115	0.5672
Couplings RH->RF CStat Mean	0.0736	0.0307	0.6338
Couplings LH->LF CStat Mean	0.2043	0.0271	0.1914
Couplings LH->RF CStat R	0.1094	0.8636	0.0400
Support Single (%)	0.9592	0.9008	0.0036
Support Girdle (%)	0.2967	0.1639	0.0118



Appendix Figure 1. *Kcnma1*^{-/-} mice show lower weight prior to CatWalk gait capture. Mouse weight the day of CatWalk assay. Unpaired Welch's t-test performed on all groups. (A) *Kcnma1*^{N999S/WT} cohort (n=10, *Kcnma1*^{WT/WT}; n=11, *Kcnma1*^{N999S/WT}). *Kcnma1*^{N999S/WT} show no significant difference to WT controls (p=0.7448) (B) *Kcnma1*^{D434G/WT} cohort (n=11, *Kcnma1*^{WT/WT}; n=9, *Kcnma1*^{D434G/WT}). *Kcnma1*^{D434G/WT} show no significant difference to WT controls (p=0.2277) (C) *Kcnma1*^{-/-} cohort (n=9, *Kcnma1*^{+/+}; n=10, *Kcnma1*^{-/-}). *Kcnma1*^{-/-} mice show lower weight (p=0.0442).

As weight differences between sex can affect paw parameters as well, cohorts were sex-matched as closely as possible. *Kcnma1*^{N999S/WT} cohort: n=5, *Kcnma1*^{WT/WT} male; n=5, *Kcnma1*^{WT/WT} female; n=6, *Kcnma1*^{N999S/WT} male; n=5, *Kcnma1*^{N999S/WT} female. *Kcnma1*^{D434G/WT} cohort: n=6, *Kcnma1*^{WT/WT} male; n=4, *Kcnma1*^{WT/WT} female; n=3, *Kcnma1*^{D434G/WT} male; n=6, *Kcnma1*^{D434G/WT} female. *Kcnma1*^{-/-} cohort: n=3, *Kcnma1*^{+/+} male; n=3, *Kcnma1*^{+/+} female; n=6, *Kcnma1*^{-/-} male; n=1, *Kcnma1*^{-/-} female.

APPENDIX 4: REPRESENTATIVE IMAGES AND VIDEO OF RESTRAINT-INDUCED DYSKINESIA BEHAVIOR



Appendix Figure 2. Representative images of *Kcnma1*^{WT/WT} and *Kcnma1*^{N999S/WT} mice. Images from restraint-induced dyskinesia video recordings. (A-B) Mice exhibiting immobility of the body, head and limbs with normal respiration. *Kcnma1*^{N999S/WT} mice show a more hunched posture. (A) *Kcnma1*^{WT/WT} mouse. (B) *Kcnma1*^{N999S/WT} mouse. (C) *Kcnma1*^{WT/WT} mouse exhibiting rearing behavior with both forelimb paws contacting the side of the beaker. (D) *Kcnma1*^{N999S/WT} mouse exhibiting grooming behavior of face and forelimbs while reared on both hindlimbs.

Appendix Video 1. Representative video of *Kcnma1*^{N999S/WT}, *Kcnma1*^{WT/WT} and *Kcnma1*^{-/-} mice. Video recordings taken 1 minute after hand restraint and placement of mice in beaker. *Left: Kcnma1*^{N999S/WT} show longer immobility with a more hunched posture with occasional myoclonus of the head and trunk. *Middle: Kcnma1*^{WT/WT} mice show some period of immobility with normal stereotypic and exploratory behavior. *Right: Kcnma1*^{-/-} mice trend towards showing hyperactivity with unsteady and jerky movements of the body, head and limbs. *Kcnma1*^{-/-} mice also trend towards showing less stereotypic behaviors.

REFERENCES

- Bailey, C.S., Moldenhauer, H.J., Park, S.M., Keros, S., and Meredith, A.L. (2019). KCNMA1-linked channelopathy. *J Gen Physiol* *151*, 1173-1189.
- Benhassine, N., and Berger, T. (2009). Large-conductance calcium-dependent potassium channels prevent dendritic excitability in neocortical pyramidal neurons. *Pflugers Arch* *457*, 1133-1145.
- Bennett, B.D., Callaway, J.C., and Wilson, C.J. (2000). Intrinsic membrane properties underlying spontaneous tonic firing in neostriatal cholinergic interneurons. *J Neurosci* *20*, 8493-8503.
- Campanari, M.L., Garcia-Ayllon, M.S., Ciura, S., Saez-Valero, J., and Kabashi, E. (2016). Neuromuscular Junction Impairment in Amyotrophic Lateral Sclerosis: Reassessing the Role of Acetylcholinesterase. *Frontiers in molecular neuroscience* *9*, 160.
- Casaca-Carreira, J., Temel, Y., van Zelst, M., and Jahanshahi, A. (2015). Coexistence of Gait Disturbances and Chorea in Experimental Huntington's Disease. *Behav Neurol* *2015*, 970204.
- Chen, W.J., Lin, Y., Xiong, Z.Q., Wei, W., Ni, W., Tan, G.H., Guo, S.L., He, J., Chen, Y.F., Zhang, Q.J., *et al.* (2011). Exome sequencing identifies truncating mutations in PRRT2 that cause paroxysmal kinesigenic dyskinesia. *Nat Genet* *43*, 1252-1255.
- Chen, X., Kovalchuk, Y., Adelsberger, H., Henning, H.A., Sausbier, M., Wietzorrek, G., Ruth, P., Yarom, Y., and Konnerth, A. (2010). Disruption of the olivo-cerebellar circuit by Purkinje neuron-specific ablation of BK channels. *Proc Natl Acad Sci U S A* *107*, 12323-12328.
- Choi, T.Y., Lee, S.H., Kim, S.J., Jo, Y., Park, C.S., and Choi, S.Y. (2018). BK channel blocker paxilline attenuates thalidomide-caused synaptic and cognitive dysfunctions in mice. *Scientific reports* *8*, 17653.
- Coffman, K.A., Dum, R.P., and Strick, P.L. (2011). Cerebellar vermis is a target of projections from the motor areas in the cerebral cortex. *Proc Natl Acad Sci U S A* *108*, 16068-16073.
- Crawley, J.N. (2000). *What's wrong with my mouse? : behavioral phenotyping of transgenic and knockout mice* (New York: Wiley-Liss).

- Diez-Sampedro, A., Silverman, W.R., Bautista, J.F., and Richerson, G.B. (2006). Mechanism of increased open probability by a mutation of the BK channel. *J Neurophysiol* *96*, 1507-1516.
- Dinardo, M.M., Camerino, G., Mele, A., Latorre, R., Conte Camerino, D., and Tricarico, D. (2012). Splicing of the rSlo gene affects the molecular composition and drug response of Ca²⁺-activated K⁺ channels in skeletal muscle. *PLoS One* *7*, e40235.
- Dong, P., Zhang, Y., Mikati, M.A., Cui, J., and Yang, H. (2021). Neuronal mechanism of a BK channelopathy in absence epilepsy and movement disorders. *BioRxiv*.
- Du, W., Bautista, J.F., Yang, H., Diez-Sampedro, A., You, S.A., Wang, L., Kotagal, P., Luders, H.O., Shi, J., Cui, J., *et al.* (2005). Calcium-sensitive potassium channelopathy in human epilepsy and paroxysmal movement disorder. *Nat Genet* *37*, 733-738.
- Duff, M.O., Olson, S., Wei, X., Garrett, S.C., Osman, A., Bolisetty, M., Plocik, A., Celniker, S.E., and Graveley, B.R. (2015). Genome-wide identification of zero nucleotide recursive splicing in *Drosophila*. *Nature* *521*, 376-379.
- Dworetzky, S.I., Trojnacki, J.T., and Gribkoff, V.K. (1994). Cloning and expression of a human large-conductance calcium-activated potassium channel. *Brain Res Mol Brain Res* *27*, 189-193.
- Ermolinsky, B., Arshadmansab, M.F., Pacheco Otalora, L.F., Zarei, M.M., and Garrido-Sanabria, E.R. (2008). Deficit of *Kcnma1* mRNA expression in the dentate gyrus of epileptic rats. *Neuroreport* *19*, 1291-1294.
- Faber, E.S., and Sah, P. (2002). Physiological role of calcium-activated potassium currents in the rat lateral amygdala. *J Neurosci* *22*, 1618-1628.
- Fagerberg, L., Hallstrom, B.M., Oksvold, P., Kampf, C., Djureinovic, D., Odeberg, J., Habuka, M., Tahmasebpoor, S., Danielsson, A., Edlund, K., *et al.* (2014). Analysis of the human tissue-specific expression by genome-wide integration of transcriptomics and antibody-based proteomics. *Mol Cell Proteomics* *13*, 397-406.
- Ford, K.J., and Davis, G.W. (2014). Archaelhodopsin voltage imaging: synaptic calcium and BK channels stabilize action potential repolarization at the *Drosophila* neuromuscular junction. *J Neurosci* *34*, 14517-14525.

Fredette, B.J., and Mugnaini, E. (1991). The GABAergic cerebello-olivary projection in the rat. *Anat Embryol (Berl)* 184, 225-243.

Fureman, B.E., Jinnah, H.A., and Hess, E.J. (2002). Triggers of paroxysmal dyskinesia in the calcium channel mouse mutant tottering. *Pharmacol Biochem Behav* 73, 631-637.

Garone, G., Capuano, A., Travaglini, L., Graziola, F., Stregapede, F., Zanni, G., Vigeveno, F., Bertini, E., and Nicita, F. (2020). Clinical and Genetic Overview of Paroxysmal Movement Disorders and Episodic Ataxias. *Int J Mol Sci* 21.

Goldberg, J.A., and Wilson, C.J. (2005). Control of spontaneous firing patterns by the selective coupling of calcium currents to calcium-activated potassium currents in striatal cholinergic interneurons. *J Neurosci* 25, 10230-10238.

Gómez, R., Maglio, L.E., Gonzalez-Hernandez, A.J., Rivero-Pérez, B., Bartolomé-Martín, D., and Giraldez, T. (2021). NMDA receptor–BK channel coupling regulates synaptic plasticity in the barrel cortex. *bioRxiv*, 2020.2012.2030.424719.

Gu, N., Vervaeke, K., and Storm, J.F. (2007). BK potassium channels facilitate high-frequency firing and cause early spike frequency adaptation in rat CA1 hippocampal pyramidal cells. *J Physiol* 580, 859-882.

He, C., Li, X., Wang, M., Zhang, S., and Liu, H. (2021). Deletion of BK channels decreased skeletal and cardiac muscle function but increased smooth muscle contraction in rats. *Biochem Biophys Res Commun* 570, 8-14.

Heim, J., Vemuri, A., Lewis, S., Guida, B., Troester, M., Keros, S., Meredith, A., and Kruer, M.C. (2020). Cataplexy in Patients Harboring the KCNMA1 p.N999S Mutation. *Movement Disorders Clinical Practice* 7, 861-862.

Hickey, M.A., Gallant, K., Gross, G.G., Levine, M.S., and Chesselet, M.F. (2005). Early behavioral deficits in R6/2 mice suitable for use in preclinical drug testing. *Neurobiol Dis* 20, 1-11.

Hickey, M.A., Kosmalska, A., Enayati, J., Cohen, R., Zeitlin, S., Levine, M.S., and Chesselet, M.F. (2008). Extensive early motor and non-motor behavioral deficits are followed by striatal neuronal loss in knock-in Huntington's disease mice. *Neuroscience* 157, 280-295.

J. Heim, A.V., S. Lewis, A. Meredith, S. Keros, M. Kruer (2019). Drop attacks in patients with KCNMA1 p.N999S heterozygous de novo mutations. 6th International Symposium on Paediatric Movement Disorders.

Kelley, A.E. (1998). Measurement of Rodent Stereotyped Behavior. *Current Protocols in Neuroscience* 4, 8.8.1-8.8.13.

Kent, J., and Meredith, A.L. (2008). BK channels regulate spontaneous action potential rhythmicity in the suprachiasmatic nucleus. *PLoS One* 3, e3884.

Keros, S., Heim, J., Hakami, W., Zohar-Dayan, E., Ben-Zeev, B., Grinspan, Z., Kruer, M.C., and Meredith, A.L. (2021). Lisdexamfetamine therapy in paroxysmal non-kinesigenic dyskinesia associated with the KCNMA1-N999S variant (MS under review).

Khan, Z., Carey, J., Park, H.J., Lehar, M., Lasker, D., and Jinnah, H.A. (2004). Abnormal motor behavior and vestibular dysfunction in the stargazer mouse mutant. *Neuroscience* 127, 785-796.

Khan, Z., and Jinnah, H.A. (2002). Paroxysmal Dyskinesias in the Lethargic Mouse Mutant. *The Journal of Neuroscience* 22, 8193-8200.

Kovoor, A., Seyffarth, P., Ebert, J., Barghshoon, S., Chen, C.K., Schwarz, S., Axelrod, J.D., Cheyette, B.N., Simon, M.I., Lester, H.A., *et al.* (2005). D2 dopamine receptors colocalize regulator of G-protein signaling 9-2 (RGS9-2) via the RGS9 DEP domain, and RGS9 knock-out mice develop dyskinesias associated with dopamine pathways. *J Neurosci* 25, 2157-2165.

Kratschmer, P., Lowe, S.A., Buhl, E., Chen, K.F., Kullmann, D.M., Pittman, A., Hodge, J.J.L., and Jepson, J.E.C. (2021). Impaired Pre-Motor Circuit Activity and Movement in a *Drosophila* Model of KCNMA1-Linked Dyskinesia. *Mov Disord*.

Künzle, H. (1975). Bilateral projections from precentral motor cortex to the putamen and other parts of the basal ganglia. An autoradiographic study in *Macaca fascicularis*. *Brain Res* 88, 195-209.

Lee, H.Y., Nakayama, J., Xu, Y., Fan, X., Karouani, M., Shen, Y., Pothos, E.N., Hess, E.J., Fu, Y.H., Edwards, R.H., *et al.* (2012). Dopamine dysregulation in a mouse model of paroxysmal nonkinesigenic dyskinesia. *The Journal of clinical investigation* 122, 507-518.

- Li, X., Poschmann, S., Chen, Q., Fazeli, W., Oundjian, N.J., Snoeijen-Schouwenaars, F.M., Fricke, O., Kamsteeg, E.J., Willemsen, M., and Wang, Q.K. (2018). De novo BK channel variant causes epilepsy by affecting voltage gating but not Ca²⁺ sensitivity. *European journal of human genetics : EJHG* 26, 220-229.
- Liu, N.N., Xie, H., Xiang-Wei, W.S., Gao, K., Wang, T.S., and Jiang, Y.W. (2019). The absence of NIPA2 enhances neural excitability through BK (big potassium) channels. *CNS Neurosci Ther* 25, 865-875.
- Mandillo, S., Heise, I., Garbugino, L., Tocchini-Valentini, G.P., Giuliani, A., Wells, S., and Nolan, P.M. (2014). Early motor deficits in mouse disease models are reliably uncovered using an automated home-cage wheel-running system: a cross-laboratory validation. *Dis Model Mech* 7, 397-407.
- Mangiarini, L., Sathasivam, K., Seller, M., Cozens, B., Harper, A., Hetherington, C., Lawton, M., Trotter, Y., Leach, H., Davies, S.W., *et al.* (1996). Exon 1 of the HD Gene with an Expanded CAG Repeat Is Sufficient to Cause a Progressive Neurological Phenotype in Transgenic Mice. *Cell* 87, 493-506.
- Maqoud, F., Cetrone, M., Mele, A., and Tricarico, D. (2017). Molecular structure and function of big calcium-activated potassium channels in skeletal muscle: pharmacological perspectives. *Physiol Genomics* 49, 306-317.
- McCobb, D.P., Fowler, N.L., Featherstone, T., Lingle, C.J., Saito, M., Krause, J.E., and Salkoff, L. (1995). A human calcium-activated potassium channel gene expressed in vascular smooth muscle. *Am J Physiol* 269, H767-777.
- McGuire, S., Chanchani, S., and Khurana, D.S. (2018). Paroxysmal Dyskinesias. *Semin Pediatr Neurol* 25, 75-81.
- Mehranfard, N., Gholamipour-Badie, H., Motamedi, F., Janahmadi, M., and Naderi, N. (2014). The effect of paxilline on early alterations of electrophysiological properties of dentate gyrus granule cells in pilocarpine-treated rats. *Iran J Pharm Res* 13, 125-132.
- Mehranfard, N., Gholamipour-Badie, H., Motamedi, F., Janahmadi, M., and Naderi, N. (2015). Long-term increases in BK potassium channel underlie increased action potential firing in dentate granule neurons following pilocarpine-induced status epilepticus in rats. *Neurosci Lett* 585, 88-91.
- Meredith, A.L., Thorneloe, K.S., Werner, M.E., Nelson, M.T., and Aldrich, R.W. (2004).

Overactive bladder and incontinence in the absence of the BK large conductance Ca^{2+} -activated K^+ channel. *J Biol Chem* 279, 36746-36752.

Meredith, A.L., Wiler, S.W., Miller, B.H., Takahashi, J.S., Fodor, A.A., Ruby, N.F., and Aldrich, R.W. (2006). BK calcium-activated potassium channels regulate circadian behavioral rhythms and pacemaker output. *Nat Neurosci* 9, 1041-1049.

Michetti, C., Castroflorio, E., Marchionni, I., Forte, N., Sterlini, B., Binda, F., Fruscione, F., Baldelli, P., Valtorta, F., Zara, F., *et al.* (2017). The PRRT2 knockout mouse recapitulates the neurological diseases associated with PRRT2 mutations. *Neurobiol Dis* 99, 66-83.

Miller, J.P., Moldenhauer, H.J., Keros, S., and Meredith, A.L. (2021). An emerging spectrum of variants and clinical features in KCNMA1-linked channelopathy. *Channels (Austin)* 15, 447-464.

Misonou, H., Menegola, M., Buchwalder, L., Park, E.W., Meredith, A., Rhodes, K.J., Aldrich, R.W., and Trimmer, J.S. (2006). Immunolocalization of the Ca^{2+} -activated K^+ channel Slo1 in axons and nerve terminals of mammalian brain and cultured neurons. *The Journal of comparative neurology* 496, 289-302.

Moldenhauer, H.J., Matychak, K.K., and Meredith, A.L. (2020). Comparative gain-of-function effects of the KCNMA1-N999S mutation on human BK channel properties. *J Neurophysiol* 123, 560-570.

Montgomery, J.R., Whitt, J.P., Wright, B.N., Lai, M.H., and Meredith, A.L. (2013). Mis-expression of the BK K^+ channel disrupts suprachiasmatic nucleus circuit rhythmicity and alters clock-controlled behavior- supplementary data. *Am J Physiol Cell Physiol* 304, C299-311.

Pallanck, L., and Ganetzky, B. (1994). Cloning and characterization of human and mouse homologs of the *Drosophila* calcium-activated potassium channel gene, slowpoke. *Human molecular genetics* 3, 1239-1243.

Pan, Y., Liu, Q., Zhang, J., Yang, Y., Tian, Y., Zeng, J., Yin, P., Mei, L., Xiong, W.C., Li, X.J., *et al.* (2020). PRRT2 frameshift mutation reduces its mRNA stability resulting loss of function in paroxysmal kinesigenic dyskinesia. *Biochem Biophys Res Commun* 522, 553-559.

Pattillo, J.M., Yazejian, B., DiGregorio, D.A., Vergara, J.L., Grinnell, A.D., and

Meriney, S.D. (2001). Contribution of presynaptic calcium-activated potassium currents to transmitter release regulation in cultured *Xenopus* nerve–muscle synapses. *Neuroscience* *102*, 229-240.

Raffaelli, G., Saviane, C., Mohajerani, M.H., Pedarzani, P., and Cherubini, E. (2004). BK potassium channels control transmitter release at CA3-CA3 synapses in the rat hippocampus. *J Physiol* *557*, 147-157.

Rainier, S. (2004). Myofibrillogenesis Regulator 1 Gene Mutations Cause Paroxysmal Dystonic Choreoathetosis. *Archives of Neurology* *61*, 1025.

Rancz, E.A., and Hausser, M. (2006). Dendritic calcium spikes are tunable triggers of cannabinoid release and short-term synaptic plasticity in cerebellar Purkinje neurons. *J Neurosci* *26*, 5428-5437.

Robertson, L., Featherby, T., Howell, S., Hughes, J., and Thomas, P. (2019). Paroxysmal and cognitive phenotypes in *Prrt2* mutant mice. *Genes, brain, and behavior* *18*, e12566.

Robitaille, R., and Charlton, M.P. (1992). Presynaptic calcium signals and transmitter release are modulated by calcium-activated potassium channels. *J Neurosci* *12*, 297-305.

Roos, R.A.C. (2010). Huntington's disease: a clinical review. *Orphanet Journal of Rare Diseases* *5*, 40.

Rueda-Orozco, P.E., and Robbe, D. (2015). The striatum multiplexes contextual and kinematic information to constrain motor habits execution. *Nat Neurosci* *18*, 453-460.

Sausbier, M., Hu, H., Arntz, C., Feil, S., Kamm, S., Adelsberger, H., Sausbier, U., Sailer, C.A., Feil, R., Hofmann, F., *et al.* (2004). Cerebellar ataxia and Purkinje cell dysfunction caused by Ca²⁺-activated K⁺ channel deficiency. *Proc Natl Acad Sci* *101*, 9474-9478.

Sausbier, U., Sausbier, M., Sailer, C.A., Arntz, C., Knaus, H.G., Neuhuber, W., and Ruth, P. (2005). Ca²⁺-activated K⁺ channels of the BK-type in the mouse brain. *Histochem Cell Biol* *125*, 725-741.

Sebastianutto, I., Maslava, N., Hopkins, C.R., and Cenci, M.A. (2016). Validation of an improved scale for rating l-DOPA-induced dyskinesia in the mouse and effects of specific dopamine receptor antagonists. *Neurobiol Dis* *96*, 156-170.

- Shao, L.R., Halvorsrud, R., Borg-Graham, L., and Storm, J.F. (1999). The role of BK-type Ca^{2+} -dependent K^{+} channels in spike broadening during repetitive firing in rat hippocampal pyramidal cells. *J Physiol* 521 Pt 1, 135-146.
- Shirley, T.L., Rao, L.M., Hess, E.J., and Jinnah, H.A. (2008). Paroxysmal dyskinesias in mice. *Mov Disord* 23, 259-264.
- Shruti, S., Clem, R.L., and Barth, A.L. (2008). A seizure-induced gain-of-function in BK channels is associated with elevated firing activity in neocortical pyramidal neurons. *Neurobiol Dis* 30, 323-330.
- Strecker, K., Adamaszek, M., Ohm, S., Wegner, F., Beck, J., and Schwarz, J. (2012). The 5-HT_{1A}-receptor agonist flibanserin reduces drug-induced dyskinesia in RGS9-deficient mice. *J Neural Transm (Vienna)* 119, 1351-1359.
- Sun, P., Wang, F., Wang, L., Zhang, Y., Yamamoto, R., Sugai, T., Zhang, Q., Wang, Z., and Kato, N. (2011). Increase in cortical pyramidal cell excitability accompanies depression-like behavior in mice: a transcranial magnetic stimulation study. *J Neurosci* 31, 16464-16472.
- Sun, P., Zhang, Q., Zhang, Y., Wang, F., Wang, L., Yamamoto, R., Sugai, T., and Kato, N. (2015). Fear conditioning suppresses large-conductance calcium-activated potassium channels in lateral amygdala neurons. *Physiol Behav* 138, 279-284.
- Tajhya, R.B., Hu, X., Tanner, M.R., Huq, R., Kongchan, N., Neilson, J.R., Rodney, G.G., Horrigan, F.T., Timchenko, L.T., and Beeton, C. (2016). Functional KCa1.1 channels are crucial for regulating the proliferation, migration and differentiation of human primary skeletal myoblasts. *Cell death & disease* 7, e2426.
- Tan, G.H., Liu, Y.Y., Wang, L., Li, K., Zhang, Z.Q., Li, H.F., Yang, Z.F., Li, Y., Li, D., Wu, M.Y., *et al.* (2018). PRRT2 deficiency induces paroxysmal kinesigenic dyskinesia by regulating synaptic transmission in cerebellum. *Cell research* 28, 90-110.
- Timotius, I.K., Canneva, F., Minakaki, G., Mocerri, S., Plank, A.C., Casadei, N., Riess, O., Winkler, J., Klucken, J., Eskofier, B., *et al.* (2019). Systematic data analysis and data mining in CatWalk gait analysis by heat mapping exemplified in rodent models for neurodegenerative diseases. *Journal of neuroscience methods* 326, 108367.
- Tricarico, D., Mele, A., and Conte Camerino, D. (2005). Phenotype-dependent functional and pharmacological properties of BK channels in skeletal muscle: effects of

microgravity. *Neurobiol Dis* 20, 296-302.

Tricarico, D., Petruzzi, R., and Camerino, D.C. (1997). Changes of the biophysical properties of calcium-activated potassium channels of rat skeletal muscle fibres during aging. *Pflügers Archiv* 434, 822-829.

Typlt, M., Mirkowski, M., Azzopardi, E., Ruettiger, L., Ruth, P., and Schmid, S. (2013). Mice with deficient BK channel function show impaired prepulse inhibition and spatial learning, but normal working and spatial reference memory. *PLoS One* 8, e81270.

Vatanpour, H., and Harvey, A.L. (1995). Modulation of acetylcholine release at mouse neuromuscular junctions by interaction of three homologous scorpion toxins with K⁺ channels. *Br J Pharmacol* 114, 1502-1506.

Veinante, P., and Deschenes, M. (2003). Single-cell study of motor cortex projections to the barrel field in rats. *The Journal of comparative neurology* 464, 98-103.

Wang, B., Rothberg, B.S., and Brenner, R. (2009). Mechanism of increased BK channel activation from a channel mutation that causes epilepsy. *J Gen Physiol* 133, 283-294.

Wang, J., Yu, S., Zhang, Q., Chen, Y., Bao, X., and Wu, X. (2017). KCNMA1 mutation in children with paroxysmal dyskinesia and epilepsy: Case report and literature review. *Translational Science of Rare Diseases* 2, 8.

Wang, X., Burke, S.R.A., Talmadge, R.J., Voss, A.A., and Rich, M.M. (2020). Depressed neuromuscular transmission causes weakness in mice lacking BK potassium channels. *J Gen Physiol* 152.

Welsh, J.P., Lang, E.J., Suglhara, I., and Llinás, R. (1995). Dynamic organization of motor control within the olivocerebellar system. *Nature* 374, 453-457.

White, R.S., Zemen, B.G., Khan, Z., Montgomery, J.R., Herrera, G.M., and Meredith, A.L. (2014). Evaluation of mouse urinary bladder smooth muscle for diurnal differences in contractile properties. *Frontiers in pharmacology* 5, 293.

Whitt, J.P., Montgomery, J.R., and Meredith, A.L. (2016). BK channel inactivation gates daytime excitability in the circadian clock. *Nature communications* 7, 10837.

Wilson, C.J., and Goldberg, J.A. (2006). Origin of the slow afterhyperpolarization and slow rhythmic bursting in striatal cholinergic interneurons. *J Neurophysiol* 95, 196-204.

Yang, J., Krishnamoorthy, G., Saxena, A., Zhang, G., Shi, J., Yang, H., Delaloye, K., Sept, D., and Cui, J. (2010). An epilepsy/dyskinesia-associated mutation enhances BK channel activation by potentiating Ca²⁺ sensing. *Neuron* 66, 871-883.

Zhang, Z.B., Tian, M.Q., Gao, K., Jiang, Y.W., and Wu, Y. (2015). De novo KCNMA1 mutations in children with early-onset paroxysmal dyskinesia and developmental delay. *Mov Disord* 30, 1290-1292.